Spin dynamics in Bi_2Se_3/ferromagnet heterostructures

Hyunsoo Yang

Electrical and Computer Engineering, National University of Singapore

eleyang@nus.edu.sg

NUS
National University
of Singapore

Outline

- Spin-orbit torque (SOT) engineering
  - Heusler alloy
  - Oxygen manipulation of SOT
  - SOT in Co/Pd and Co/Ni multilayers
  - AHE & SOT in $LaAlO_3/SrTiO_3$ oxide heterostructures
  - SOT in topological insulators (Bi_2Se_3/ferromagnet)

NUS National University of Singapore

Charge electronics → Spin electronics

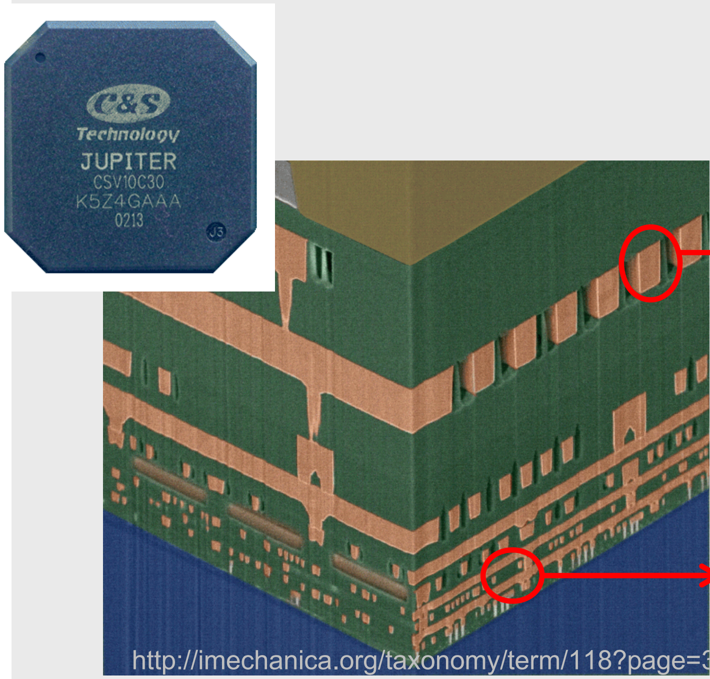

Information transfer

= electron transfer

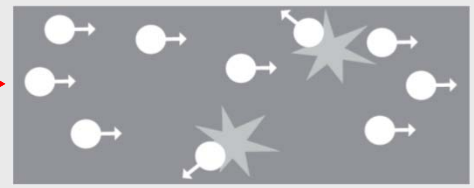

Information processing

= processing electron flow

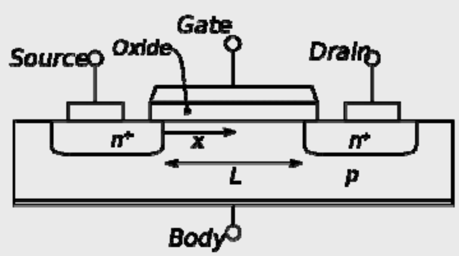

Spin waves

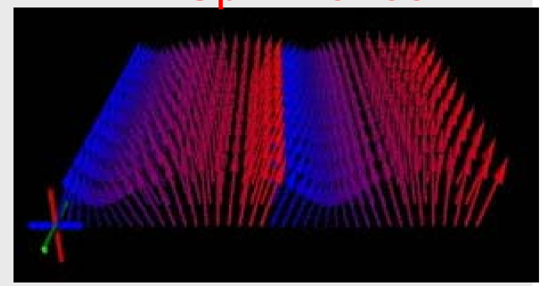

MTJs

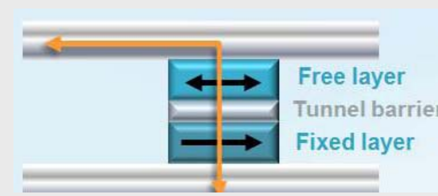

Spin transistor

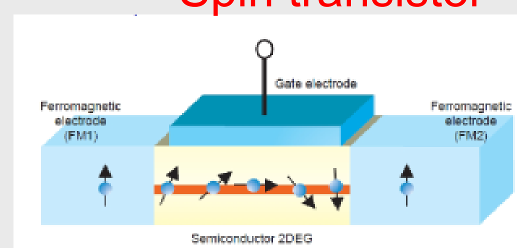

Charge transfer and processing energy loss is huge
→ All spin electroinics

Spin-orbit torques (SOT)

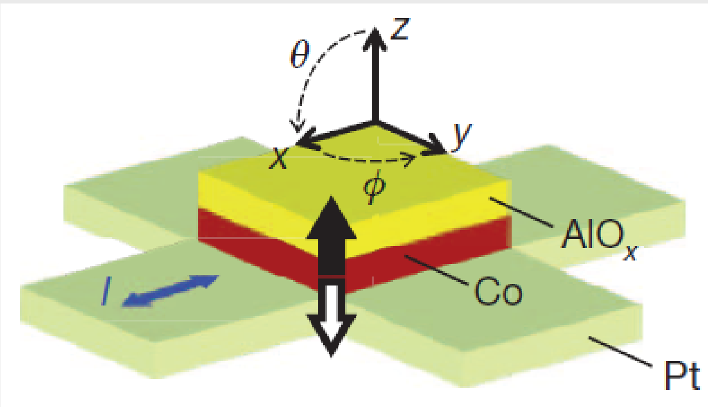

Miron *et al*. Nature **476**, 189 (2011)

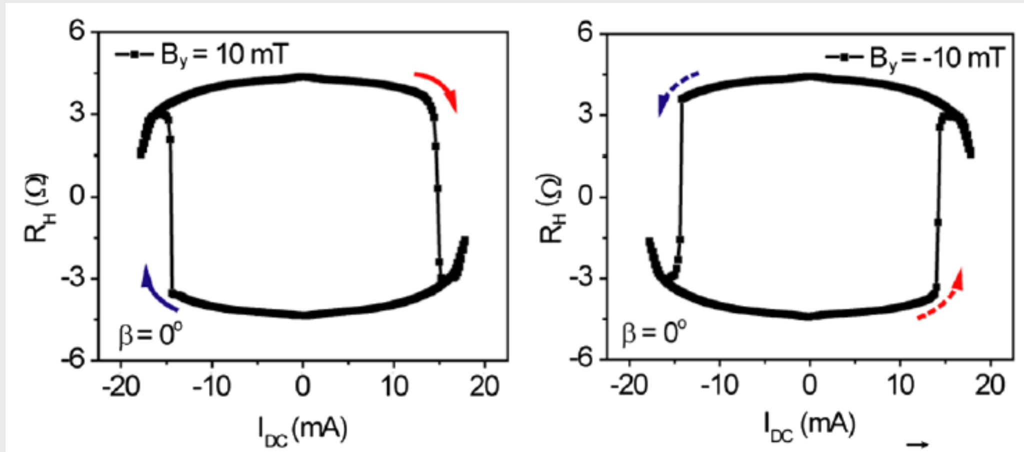

Liu *et al.* PRL **109**, 096602 (2012)

- Heavy metal/ferromagnetic material/oxide layer.
- Current induced magnetization switching is observed (longitudinal field needed).
- Magnetization states depend on both current and field directions.
- Possible mechanisms: Rashba effect & spin Hall effect (SHE).

Perpendicularly magnetized trilayer structures

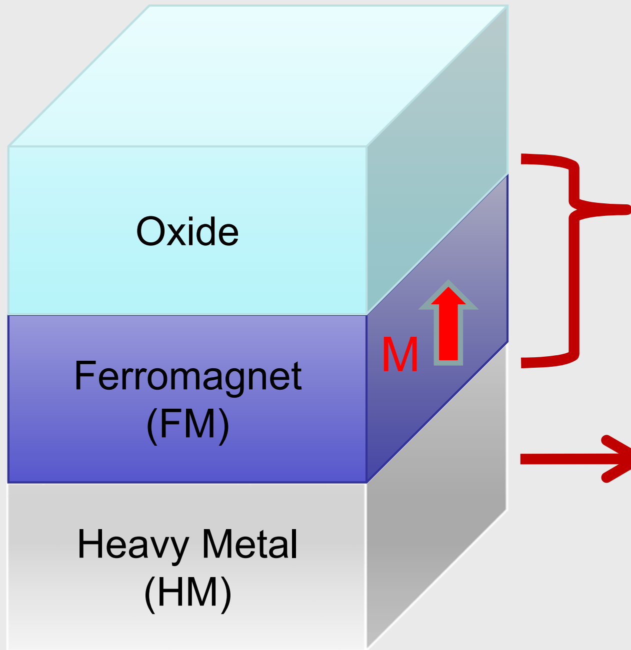

Strong Rashba field arises from asymmetric interfaces

Spin Hall effect arises from HM

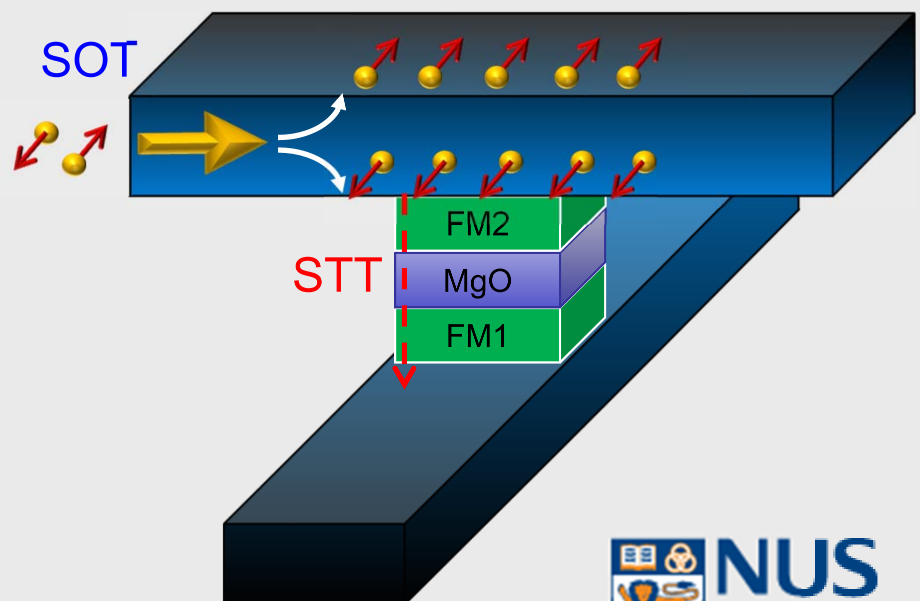

In-plane currents can switch the magnetization

Spin Hall vs. interfacial Rashba

Reverse switching polarity by oxygen engineering

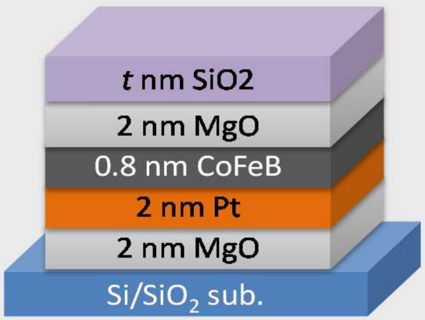

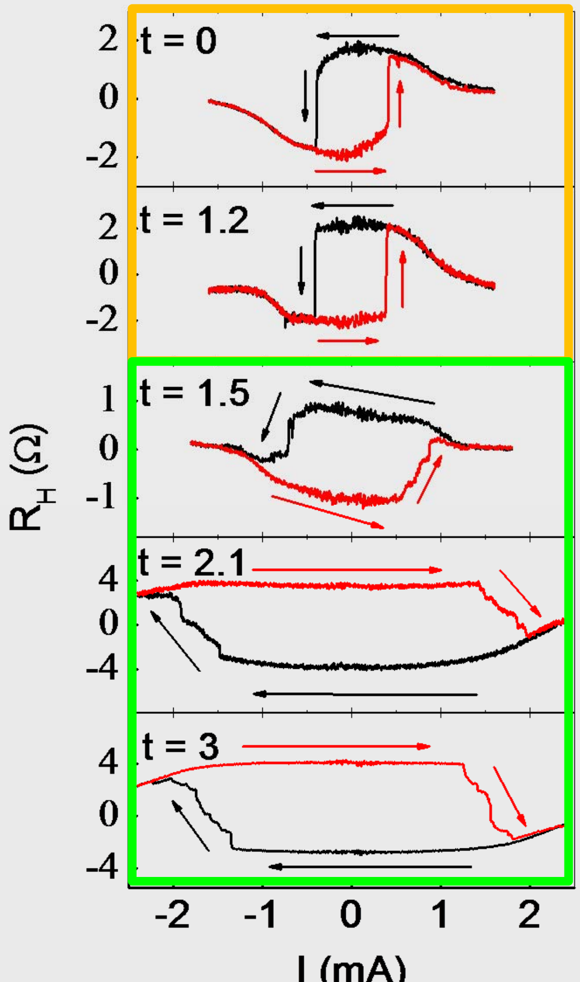

$\theta_{SH} < 0$

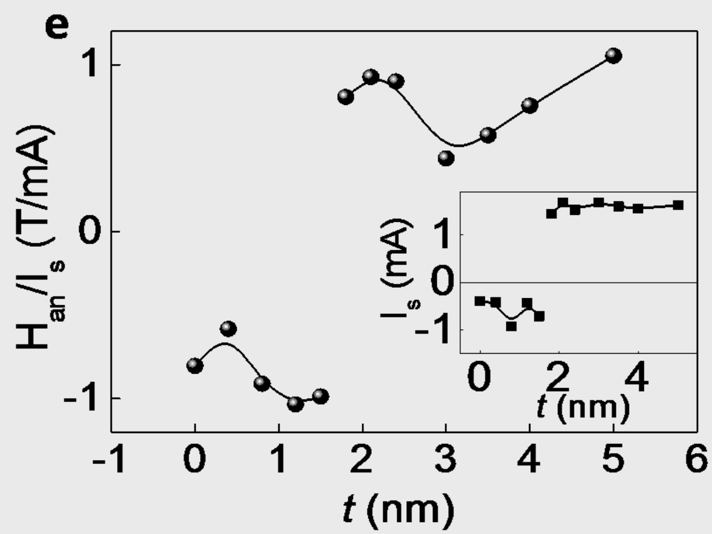

$\theta_{SH} > 0$

-Sign of spin Hall angle changes across a transition thickness of SiO_2 (t = 1.5 nm)

-Cannot be understood by spin Hall physics → suggest the role of interface

Nat. Nanotech. **10**, 333 (2015)

Spin-orbit torque switching currents

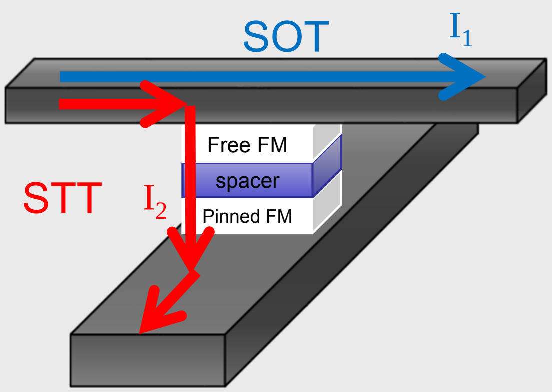

$$I_c \approx \frac{2e}{\hbar}\left(\frac{\alpha M_S V}{\eta P}\right) H_{eff} \quad \text{STT}$$

$$I_c \approx \frac{e}{\hbar}\left(\frac{M_S t_{FM} A_{HM}}{\theta_{SH}}\right) H_{eff} \quad \text{SOT}$$

K.J.Lee, APL (2013)

-No damping term → great flexibility for choosing FM, high speed

-No spin polarization term → no need to use MgO

-Can use thick MgO→ eliminate MgO breakdown issue

-Large spin Hall angle (θ_{SH}) or effective field (H_{eff}) is the key

$$H_{eff} = \hbar\theta_{SH}|j_e|/(2|e|M_S t_F)$$

Large spin Hall angles from various materials

FePt/Au spin Hall angle (θ_{SH}) = 0.1 (Takanashi group)

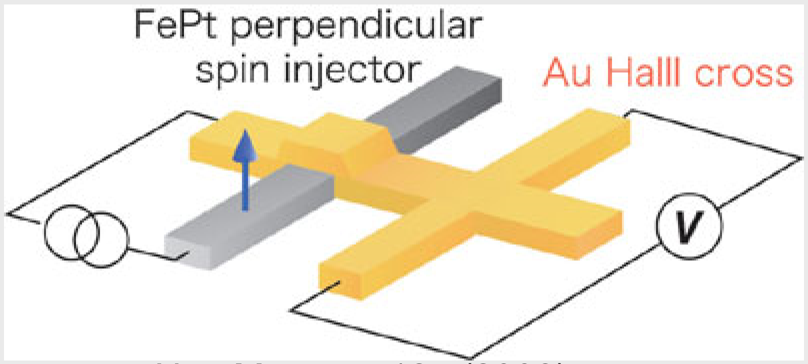

Nat. Mater. 7, 125 (2008)

CuBi θ_{SH} = -0.24 (Otani group)

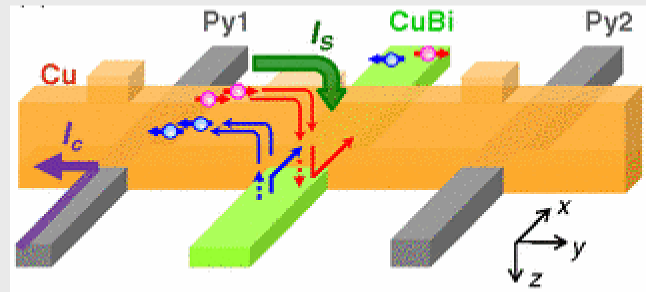

Phys. Rev. Lett. 109, 156602 (2012)

β-W θ_{SH} = 0.3 (Cornell)

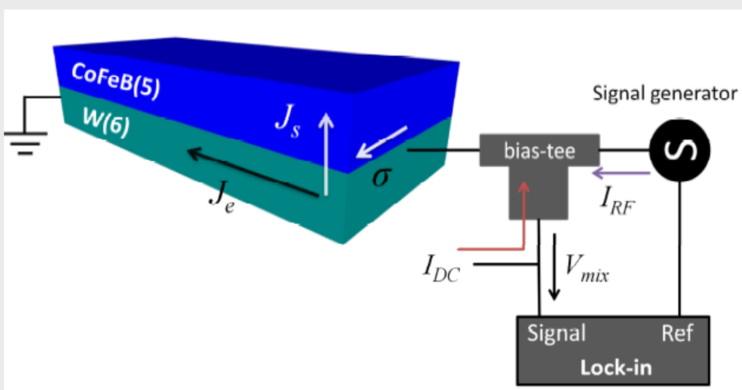

Appl. Phys. Lett. 101, 122404 (2012)

Co/Pd multilayer θ_{SH} = 4 (NUS)

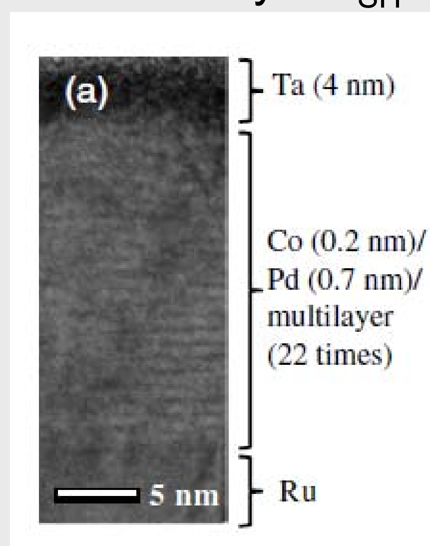

Phys. Rev. Lett. **111**, 246602 (2013)

Spin orbit torque from Heusler alloy

$Pt/Co_2FeAl_{0.5}Si_{0.5}$ (0.8 nm)/MgO

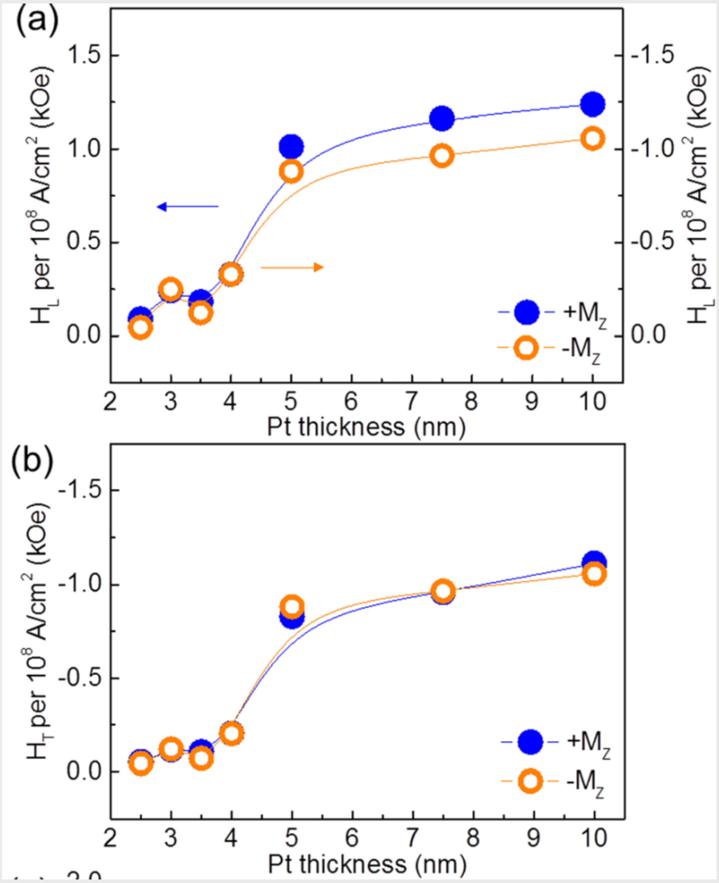

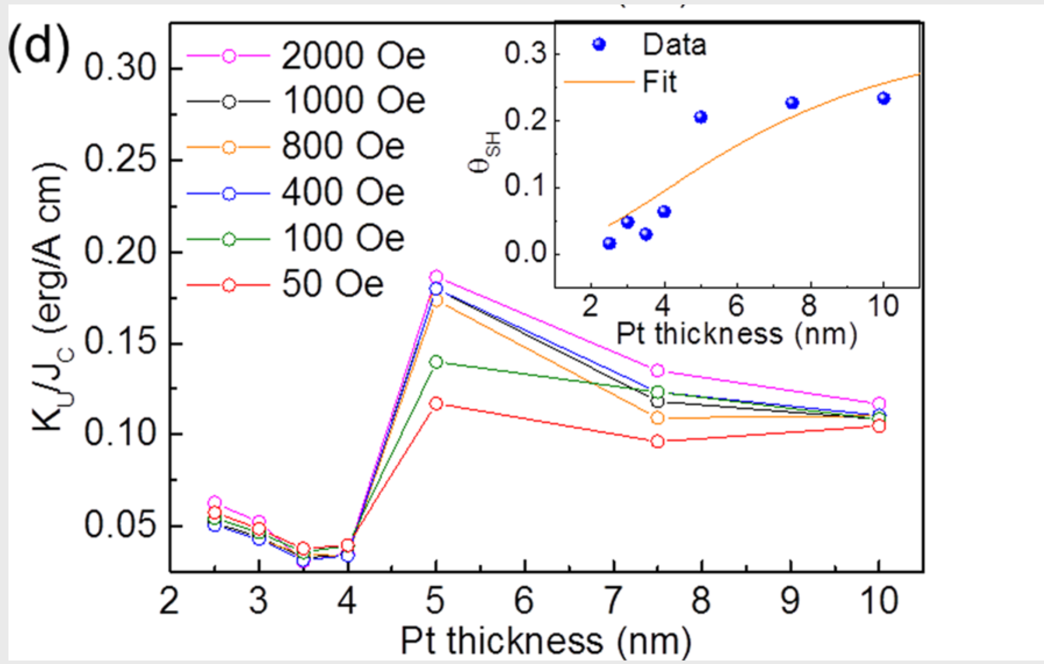

- Perpendicular anisotropy CFAS
- Both H_L and H_T exist with a large θ_{SH}

Appl. Phys. Lett. **107**, 022405 (2015)

Single magnetic layer vs. magnetic multilayer systems

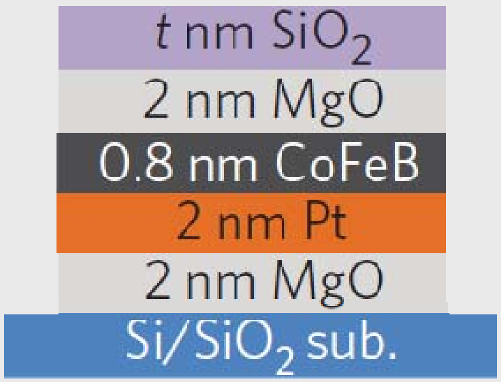

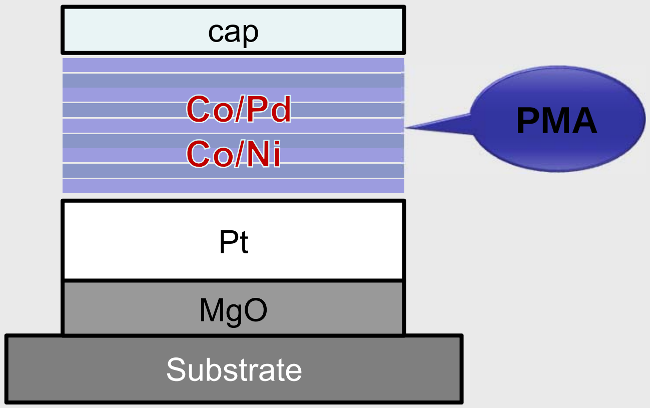

A better choice for structural engineering

- Perpendicular magnetic anisotropy (PMA) originates from Pt/FM interface.
- Low damping (~0.02)
- Spin polarization (~50%)
- Low thermal stability (not enough volume)

- Co/Pd or Co/Ni interfaces contribute to PMA.
- Lower damping (~0.01)
- Higher spin polarization (~80%)
- Good thermal stability [$\Delta = K_u V/(k_B T)$]

NUS National University of Singapore

Spin orbit torques in Co/Pd multilayers

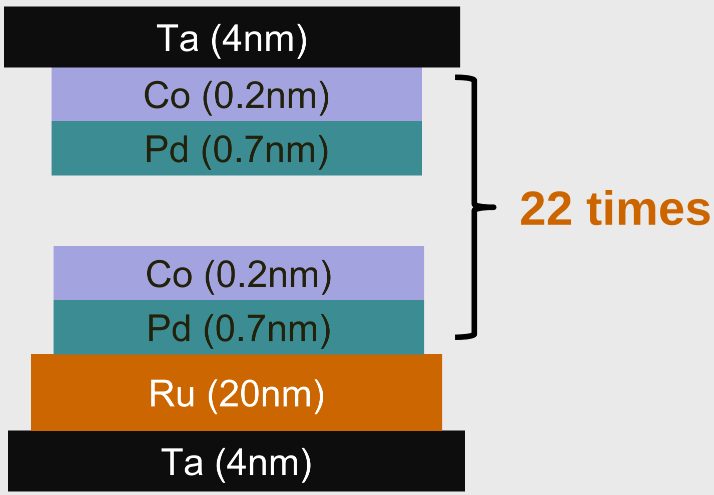

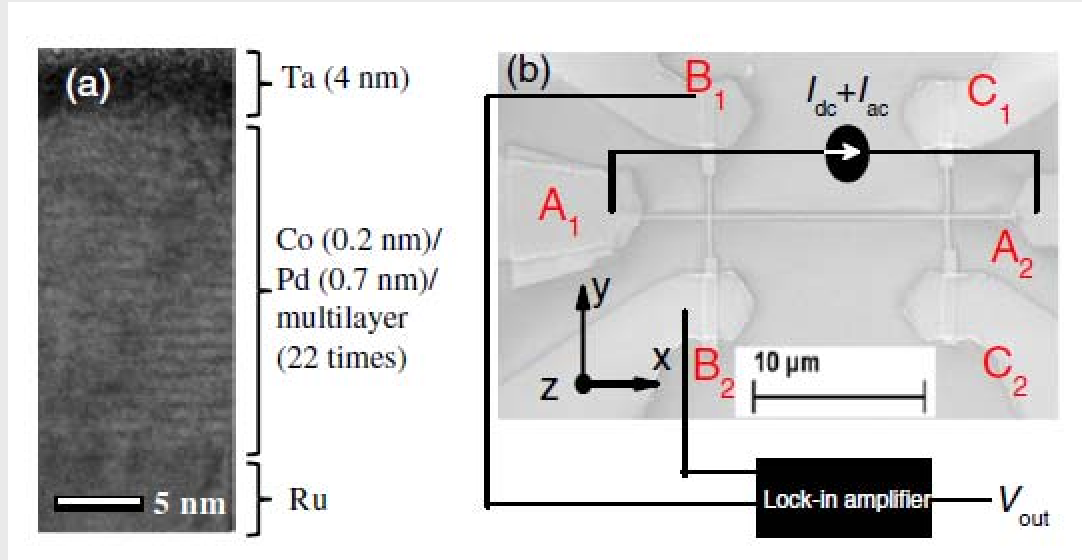

TABLE I. Summary of the reported longitudinal and transverse torque components and the extracted dimensionless coefficients. The values in the brackets indicate the corresponding effective efficiency $\alpha_{\parallel,\perp}$. For the present work we used $t = 20$ nm and $M_S = 6.23 \times 10^5$ A/m. Note that the torques from Ref. [27] are taken at $\theta = 0$.

Structure (nm)	$\beta_\parallel$ (Oe/10^8 A/cm^2) [$\alpha_\parallel$]	$\beta_\perp$(Oe/10^8 A/cm^2) [$\alpha_\perp$]	$\beta_\perp/\beta_\parallel$	Ref.
Ta(4)/$Co_{40}Fe_{40}B_{20}$(1)/MgO(1.6)	350 [0.12]	-		[6]
Ta(3)/$Co_{40}Fe_{40}B_{20}$(0.9)/MgO(2)	240 [0.07]	450 [0.13]	1.9	[27]
Ta(1.5)/$Co_{40}Fe_{40}B_{20}$(1)/MgO(1.6)	135 [0.078]	472 [0.27]	4	[10]
Pt(3)/Co(0.6)/AlO_x(1.6)	690 [0.13]	400 [0.073]	0.58	[27]
Ta(4)/Ru(20)/$(Co/Pd)_{22}$/Ta(4)	1170 [4.4]	5025 [19.1]	4.3	This work

Phys. Rev. Lett. **111**, 246602 (2013)

Structural asymmetry can be added up

TEM data

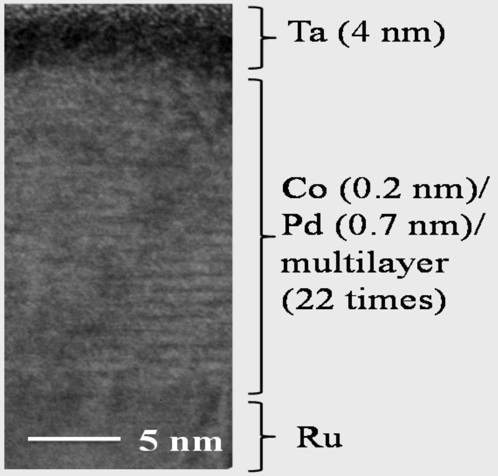

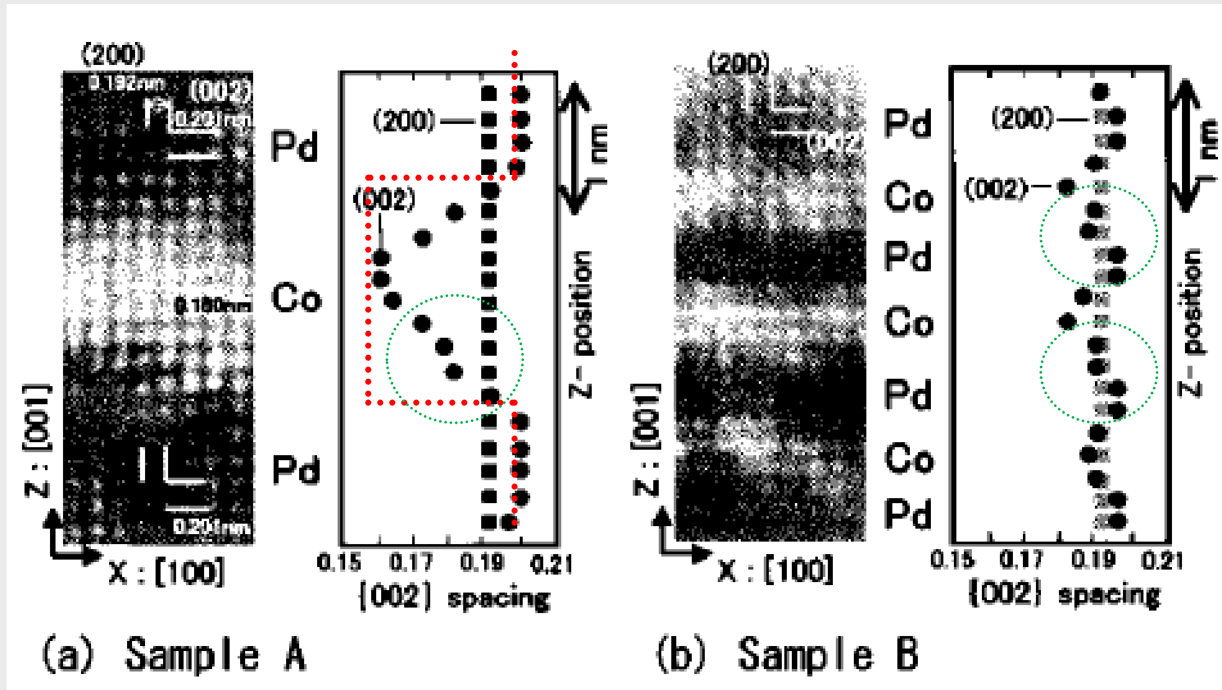

Maesaka, IEEE Trans. Magn. 38, 2676 (2002)

-Two successive Co/Pd and Pd/Co interfaces are structurally dissimilar.

-Lattice mismatch (9%) between Pd and Co

NUS National University of Singapore

LAO/STO – 2DEG formation

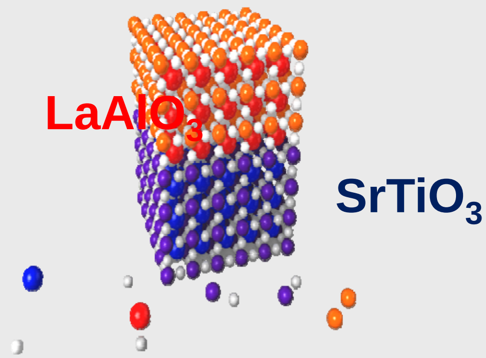

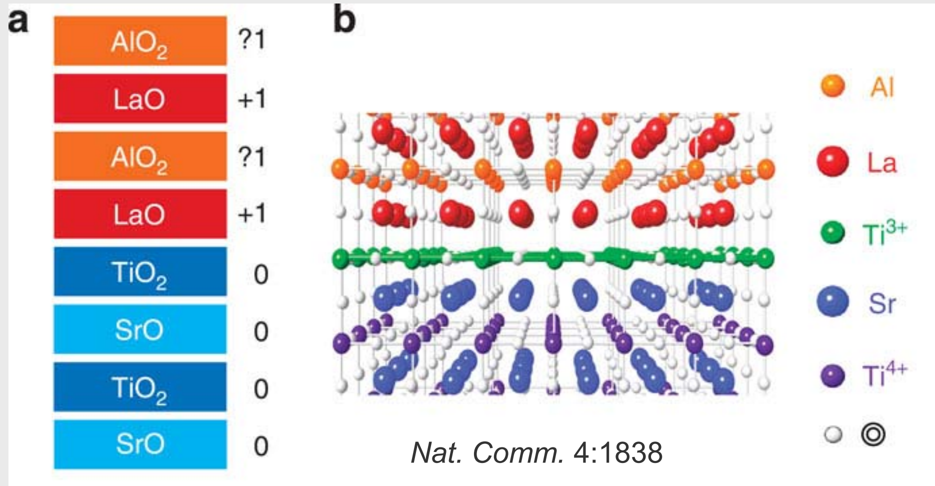

$LaAlO_3$ grown on TiO_2 terminated $SrTiO_3$ (100)

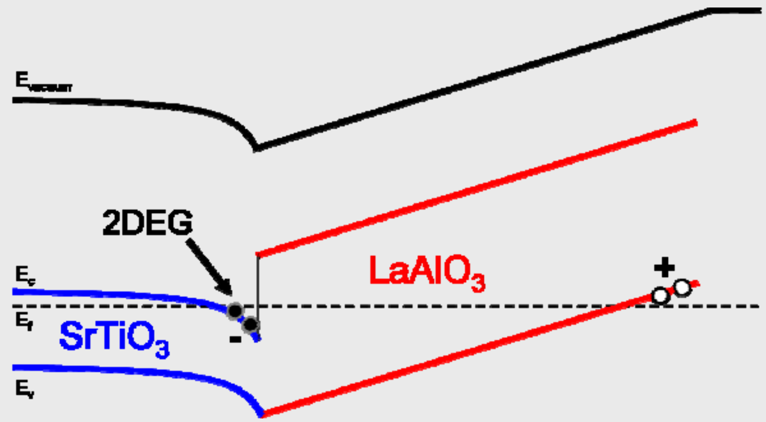

- ❑ $SrTiO_3$ (Insulator 3.2 eV)
- ❑ $LaAlO_3$ (Insulator 5.6 eV)

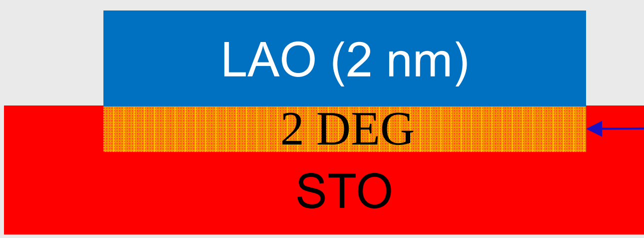

2 DEG formed inside the STO side

Magnetism in $LaAlO_3/SrTiO_3$ heterostructures

In-plane angular measurements

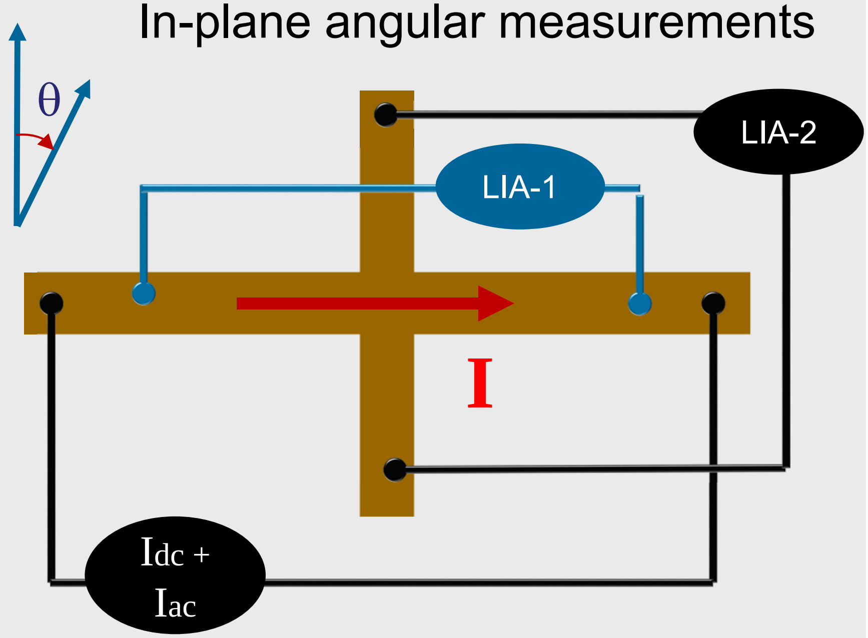

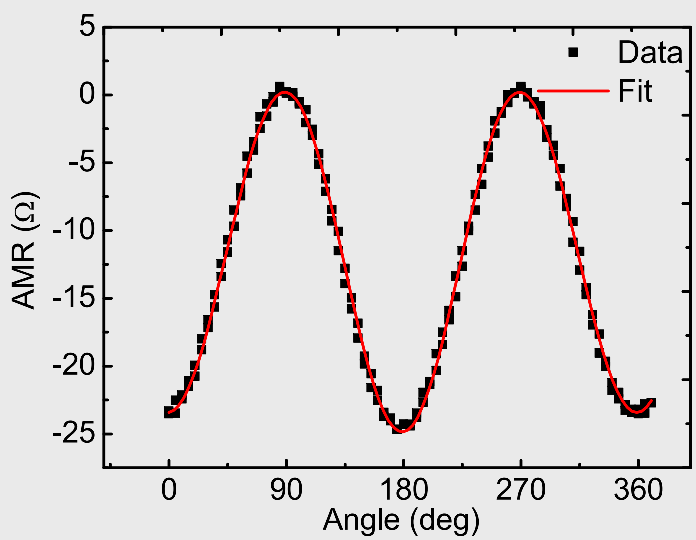

AMR measurements at H = 9 T , T = 4 K

$$R_{XX} = a_0 + a_1\cos^2(\theta+\phi) + a_2\cos^4(\theta+\phi)$$

a_0, a_1, a_2 are constants

NUS National University of Singapore

Appl. Phys. Lett. 105, 162405 (2014)

Asymmetric spin-orbit fields

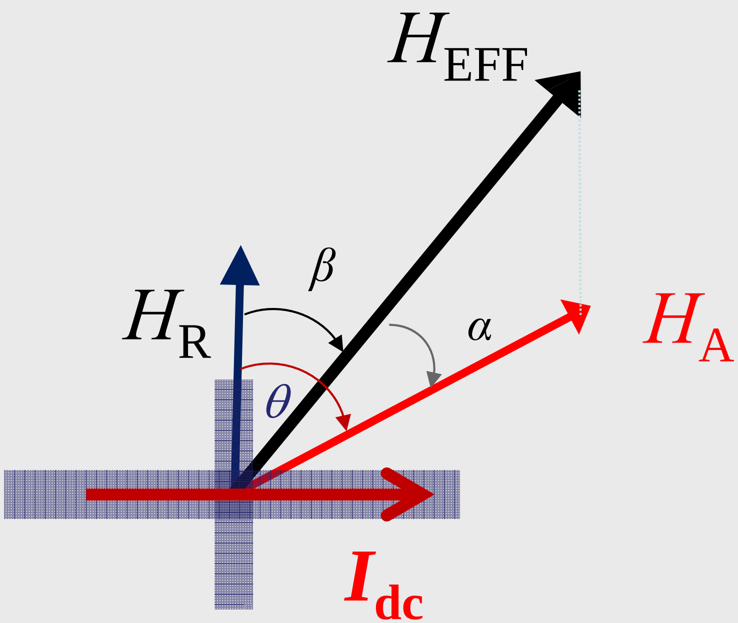

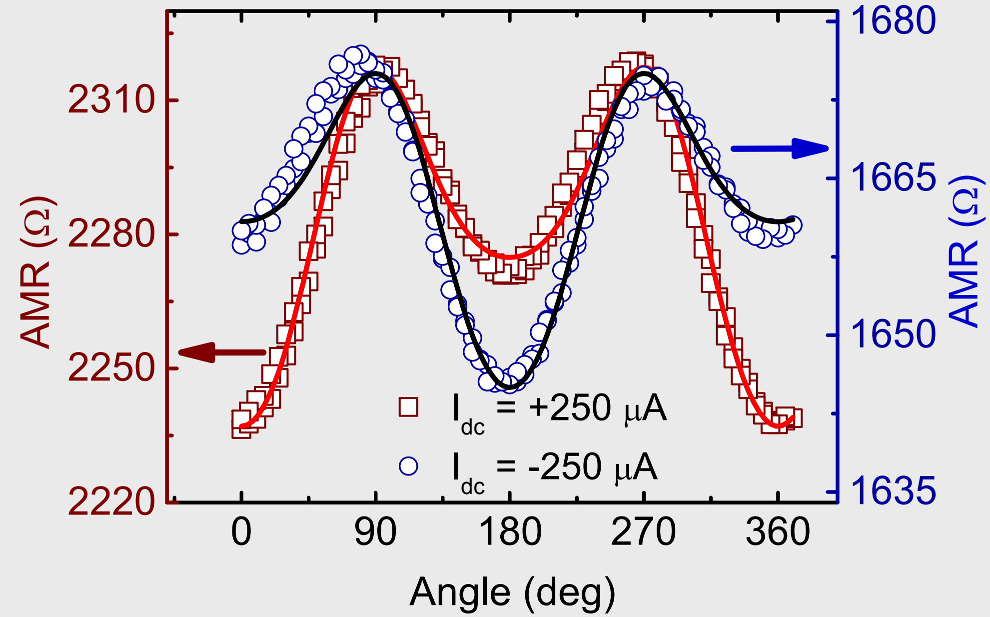

$$H_{EFF}{}^2 = H_A{}^2 + H_R{}^2 + 2H_A H_R \cos\theta$$

$$R_{XX} = b_0 + b_1 \mathrm{H}_{EFF} \cos^2\alpha + b_2 \mathrm{H}_{EFF} \cos^4\alpha$$

$H_R(+I)$ = 1.26 T
$H_R(-I)$ = -1.48 T

H_R, H_A H_{EFF} are Rashba, applied and effective fields

b_0, b_1, b_2 are constants

Appl. Phys. Lett. 105, 162405 (2014)

Current induced spin-orbit fields in 2DEG

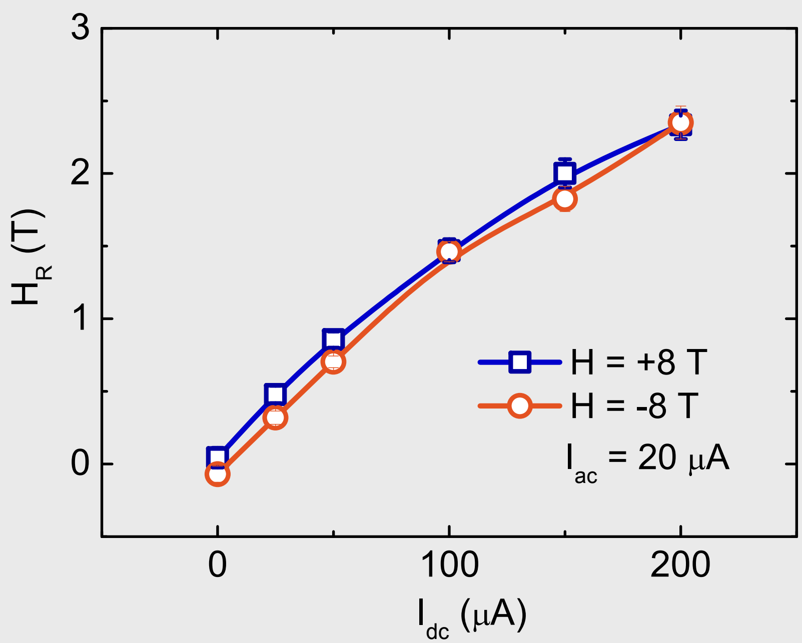

Assuming thickness of 2DEG
t_{2DEG} = 7 nm
Nat. Mater. **7**, 621 (2008)

current density = 7.14×10^8 A/m^2

2.35 T @ 200 μA
→ **32.9** Tesla/10^6 A/cm^2

The highest current induced torque reported in metallic system is only 0.5 T.

PRL **111**, 246602 (2013)

$$\alpha_R = \sqrt{\hbar^3 e H_{so} / m^{*2}}$$

H_{so} = 1.48 T, α_R = 12 meV·Å, spin splitting Δ = 3 meV (~30 T)

cf. Co/Pd multilayer α_R =360 meV·Å

NUS National University of Singapore

Appl. Phys. Lett. 105, 162405 (2014)

Magnetism imaging in LAO/STO by Squid

Squid data

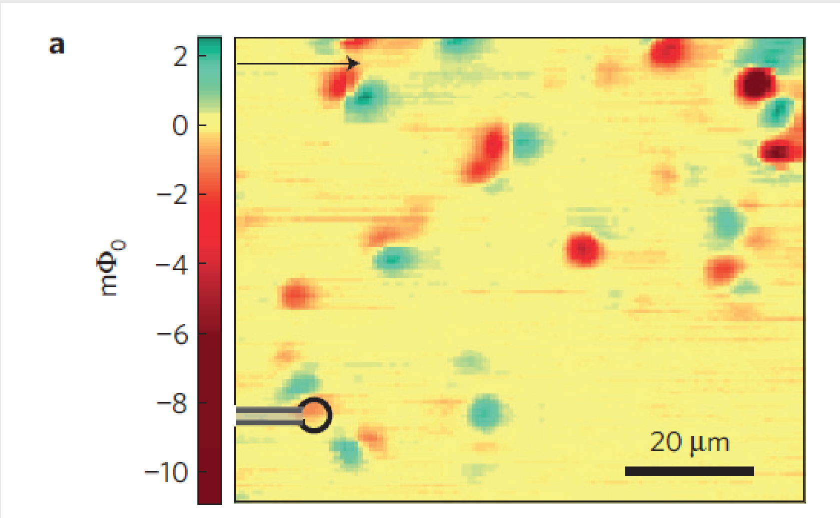

Nat. Phys. 7, 771 (2011)

10 u.c. $LaAlO_3$

TiO_2-terminated 001 STO substrates

n-type similar to our samples

Magnetic dipoles from LAO/STO

→ Squid magnetometry is sensitive to the stray field.

NUS National University of Singapore

Magnetism imaging in LAO/STO structures by MFM

MFM images

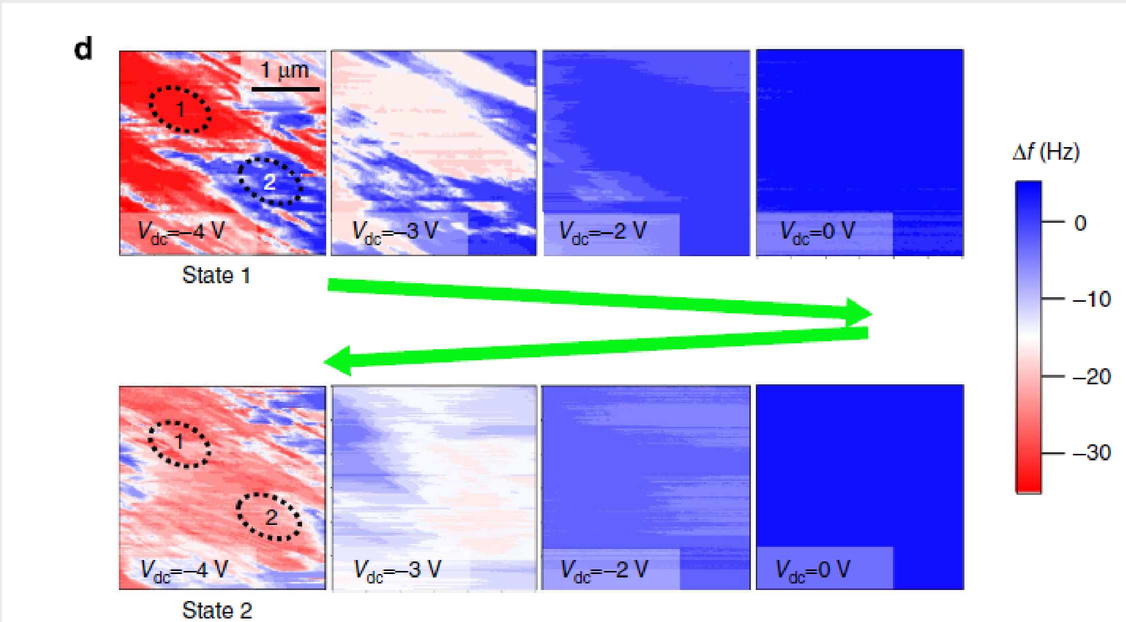

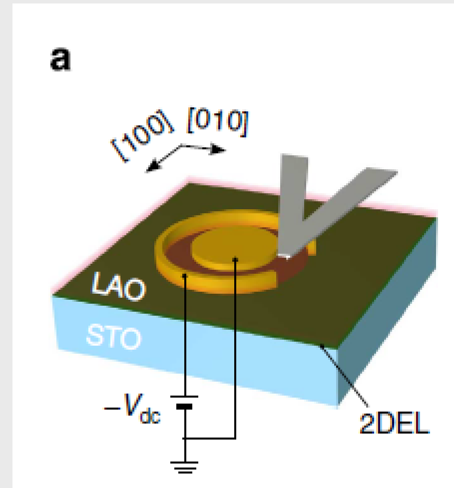

Nat. Comm. **5**, 5019 (2014).

12 unit cell LAO films on TiO_2-terminated (001) STO substrates

→ Ferromagnetism arises at lower gate voltages when the 2DEG is depleted.

Microscopic mechanism of the anomalous Hall effect

1. Intrinsic

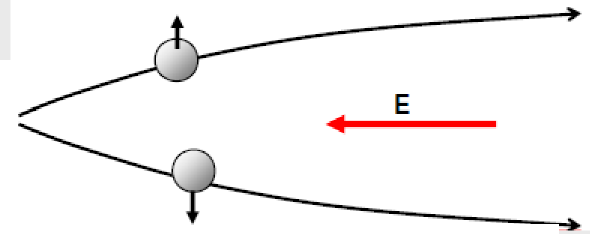

Berry Phase → Electrons have an anomalous velocity perpendicular to the electric field related to their Berry's phase curvature

2. Extrinsic

Side jump → deflection by the opposite electric fields experienced upon approaching and leaving an impurity.

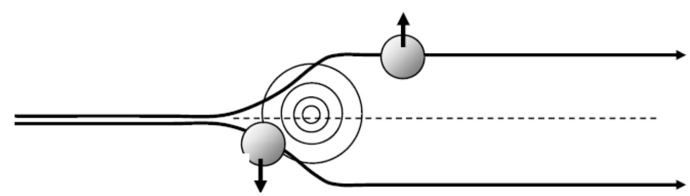

Skew → Asymmetric scattering due to the effective spin-orbit coupling of the electron or the impurity.

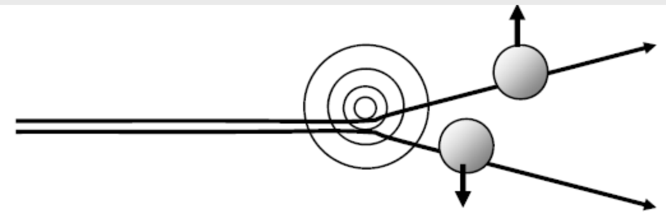

NUS National University of Singapore

Topological insulators (TIs)

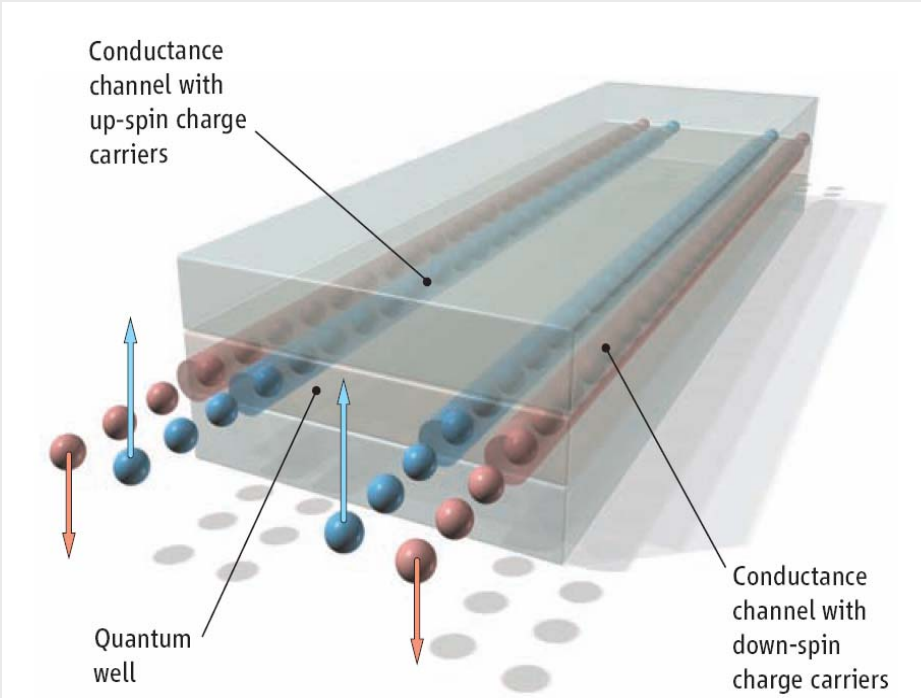

Schematic of the spin-polarized edge channels in a quantum spin Hall insulator.

Nobel Symposium 2010, Shoucheng Zhang

- ❑ Spin polarized surface currents

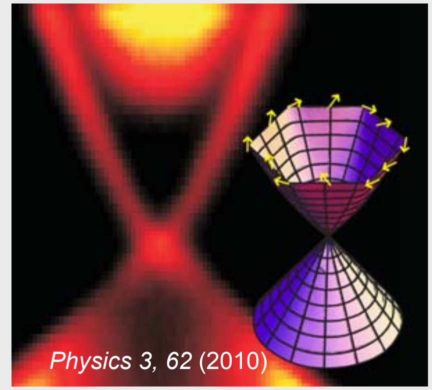

ARPES spectra showing a linear band structure of the surface states on a 3D TI

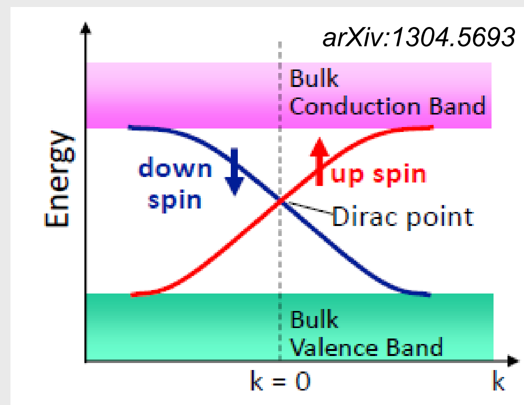

- ❑ Linear dispersion

Spin pumping

A schematic describing spin pumping

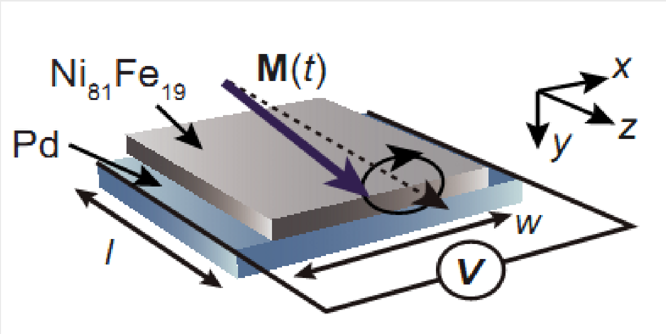

Enhancement of Gilbert damping

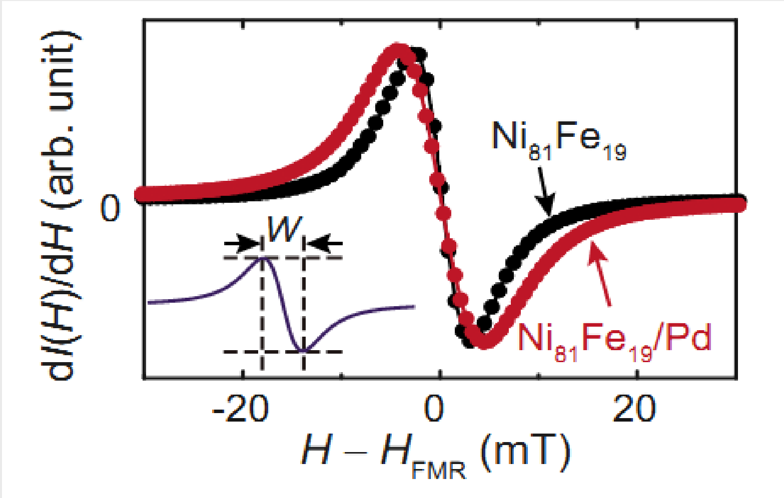

J. Appl. Phys. **108**, 113925 (2010)

Spin pumping is a process in which a precessing magnetization induces spin currents into an adjacent magnetic layer

Tserkovnyak *et al*., Phys. Rev. Lett. **88**, 117601 (2002)

Experimental setup

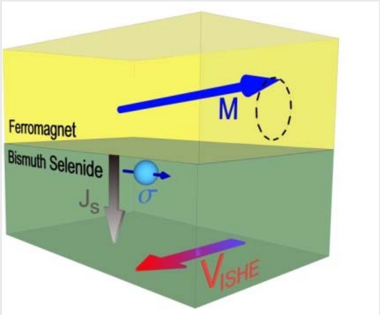

Magnetization oscillation provides high density spin currents into TI and a transverse voltage is detected in TI spin detector.

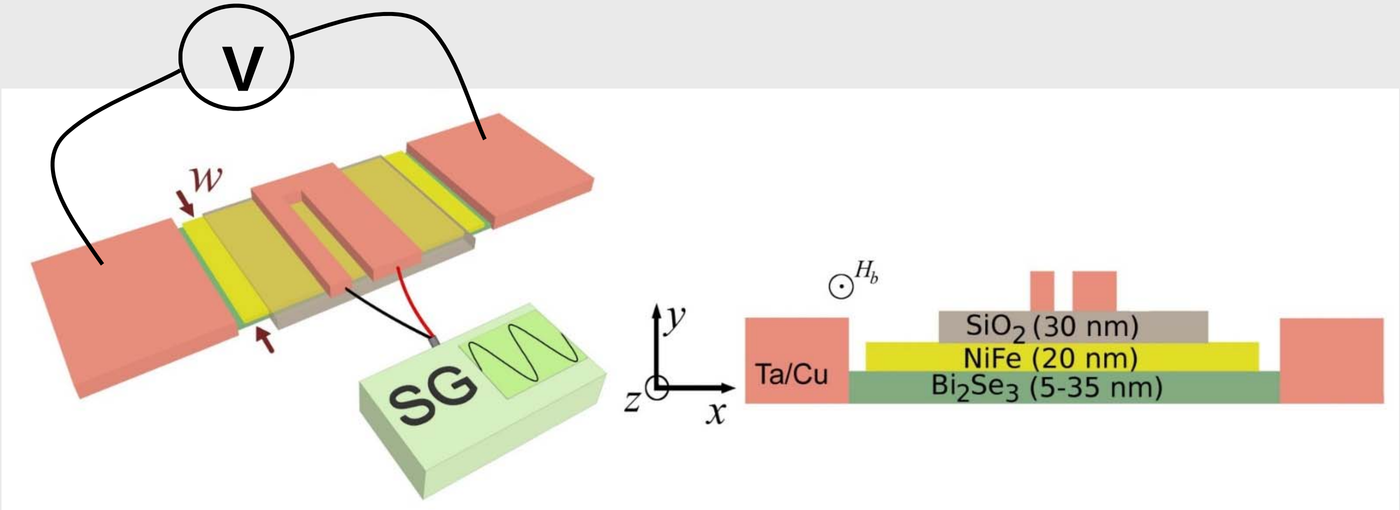

- Signal generator to excite magnetization dynamics in NiFe through a coplanar waveguide
- Voltmeter to measure spin pumping induced ISHE
- Vector network analyzer for FMR measurements

Phys. Rev. B **90**, 094403 (2014)

Characterization of Bi_2Se_3

Resistivity of 20 QL Bi_2Se_3

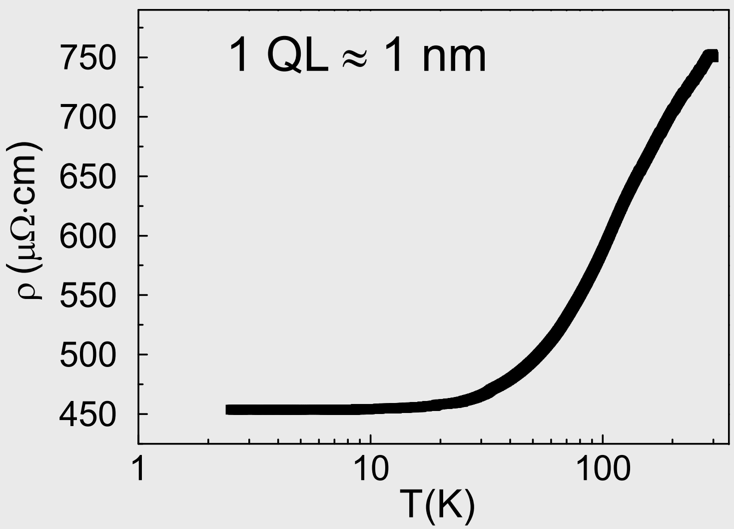

Carrier concentration of 20 QL Bi_2Se_3

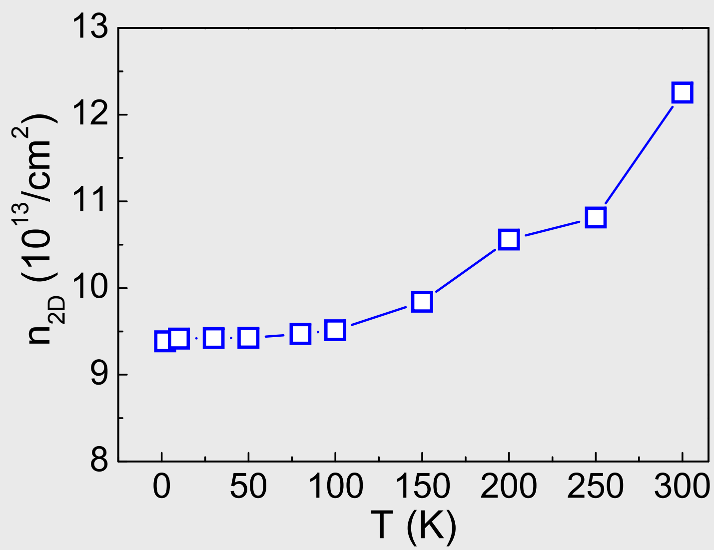

Show a typical Bi_2Se_3 feature of saturation below 30 K.

Appl. Phys. Lett. **103**, 213114 (2013)

FMR measurements

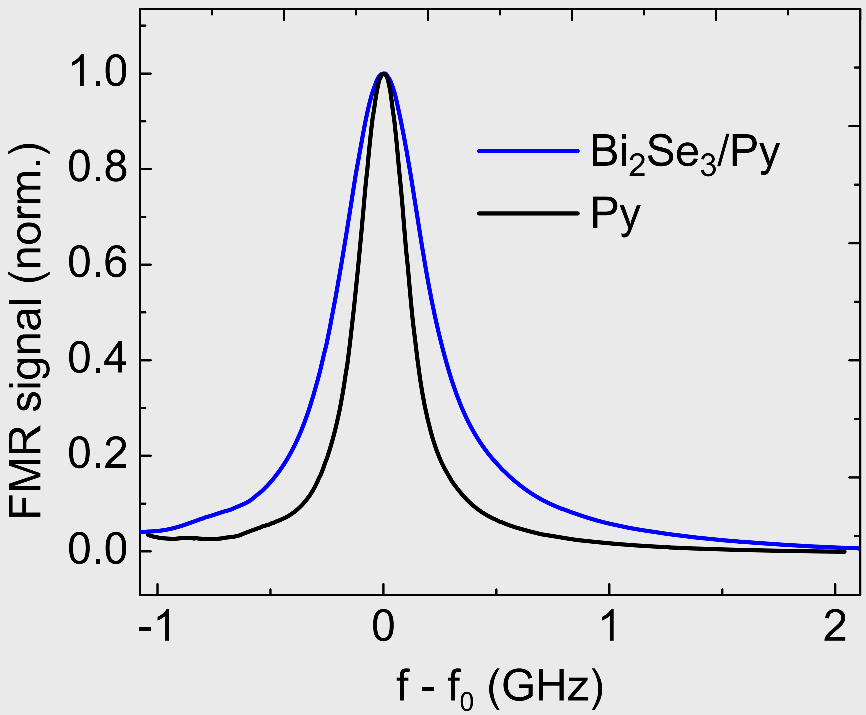

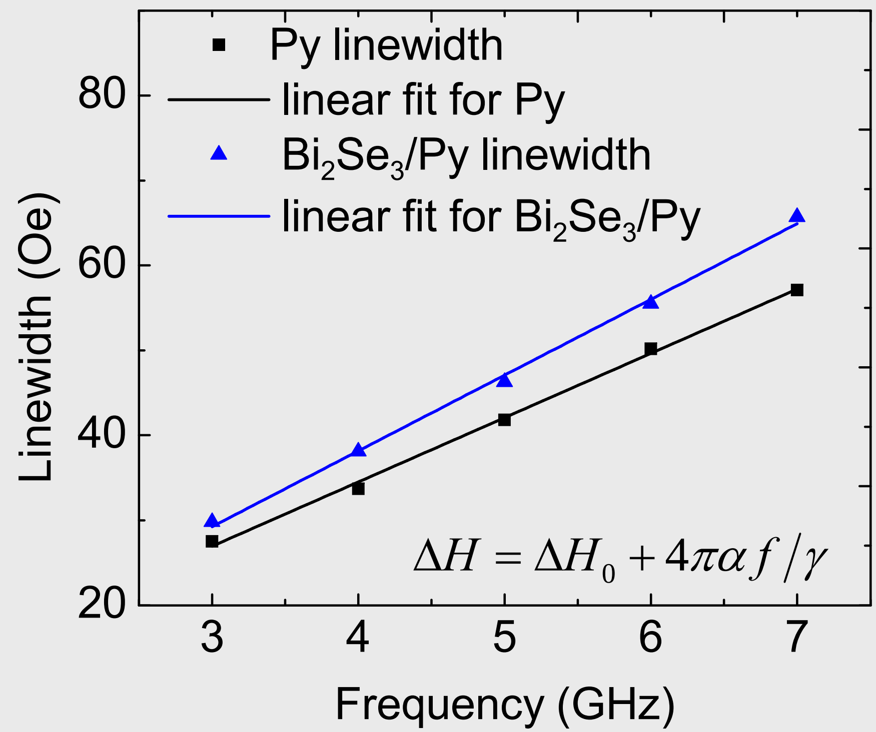

Increase in linewidth is indicative of spin pumping.

$$g_{r\uparrow\downarrow} = 4\pi M d_{Py} (\Delta\alpha)/(g\,\mu_B) \quad \Longrightarrow \quad g_{r\uparrow\downarrow} = 1.514\times10^{19}\ \mathrm{m}^{-2}$$

Phys. Rev. B **90**, 094403 (2014)

ISHE measurements

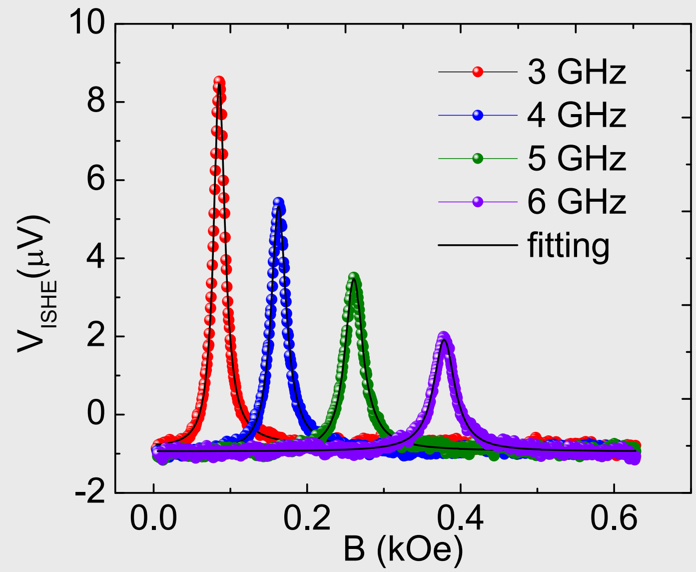

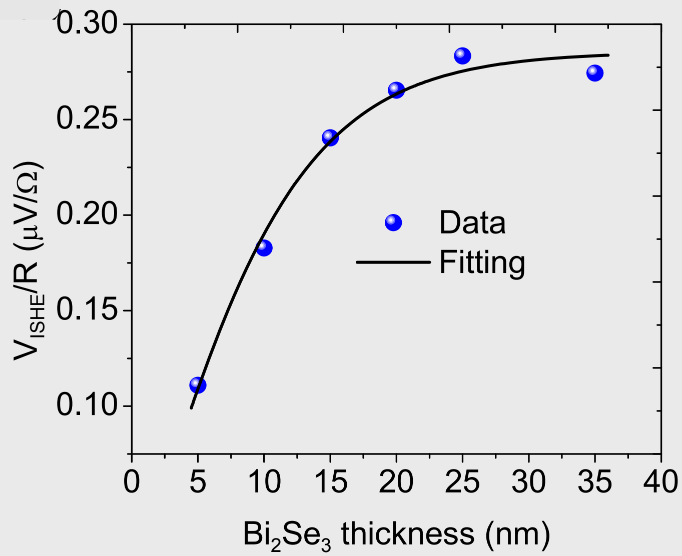

$V_{ISHE} \sim R \cdot J_s \cdot \theta_{SH}$

$$\frac{V_{ISHE}}{R} = \theta_{sh} w d_{BiSe} \left(\frac{2e}{\hbar}\right) \frac{\hbar g_{r\uparrow\downarrow} \gamma^2 h_{rf}^2 \left(M\gamma + \sqrt{M^2\gamma^2 + 4\omega^2}\right)}{8\pi\alpha^2 \left(M^2\gamma^2 + 4\omega^2\right)} \frac{\lambda_{sf}}{d_{BiSe}} \tanh\left(\frac{d_{BiSe}}{2\lambda_{sf}}\right)$$

R is resistance of the film

J_s is induced spin current

θ_{SH} is spin Hall angle

⇨ $\theta_{sh} = 0.01$

$\lambda_{sf} = 6.2$ nm

Phys. Rev. B **90**, 094403 (2014)

NUS National University of Singapore

Weak anti-localization in Bi_2Se_3

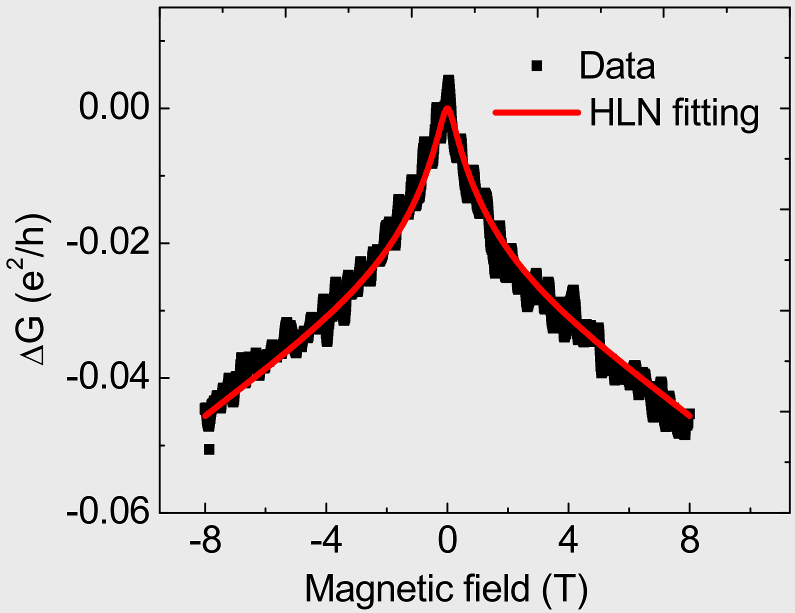

$$\Delta G(B) = -\frac{\alpha e^2}{\pi h}\left[\psi\left(\frac{\hbar}{4eL^2B}+\frac{1}{2}\right)-\ln\left(\frac{\hbar}{4eL^2B}\right)\right]+\beta B^2$$

$$\beta = \beta_c + \beta_q$$

$$\beta_c = -\mu_H^2 G_0$$

$$\beta_q = -\frac{e^2}{24\pi h}\left[\frac{1}{B_{so}+B_e}\right]^2 + \frac{3e^2}{48\pi h}\left[\frac{1}{(4/3)B_{so}+B_\phi}\right]^2$$

$$B_{so} = \hbar/\left(4el_{so}^2\right)$$

$$B_e = \hbar/\left(4el_e^2\right)$$

Taking l_e = 10 nm, spin orbit length l_{so} was found to be 6.9 nm

➔ $l_{so} \sim \lambda_{sf}$ suggest that spin-orbit coupling is dominant source of spin scattering

Phys. Rev. B **90**, 094403 (2014)

Temperature dependence

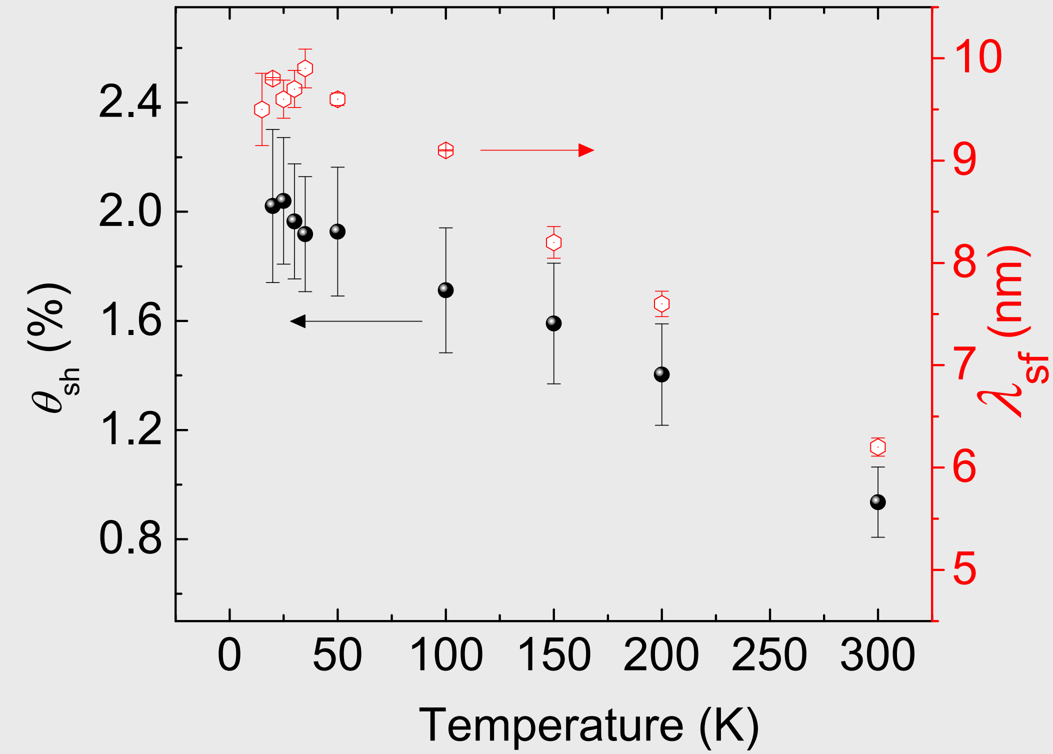

- Both spin Hall angle and spin diffusion length increase at low temperature
- θ_{sh} = 0.022 and λ_{sf} = 9.5 nm at 15 K

Phys. Rev. B **90**, 094403 (2014)

Bulk spin relaxation time in Bi_2Se_3

Time-resolved magneto optical Kerr effect

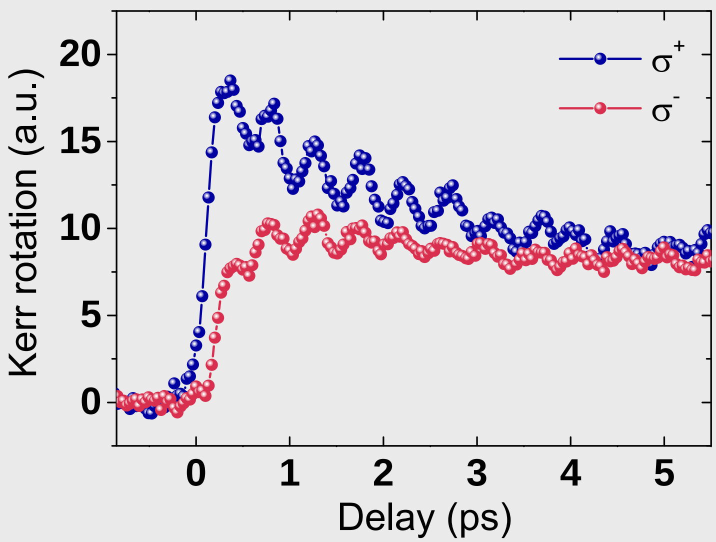

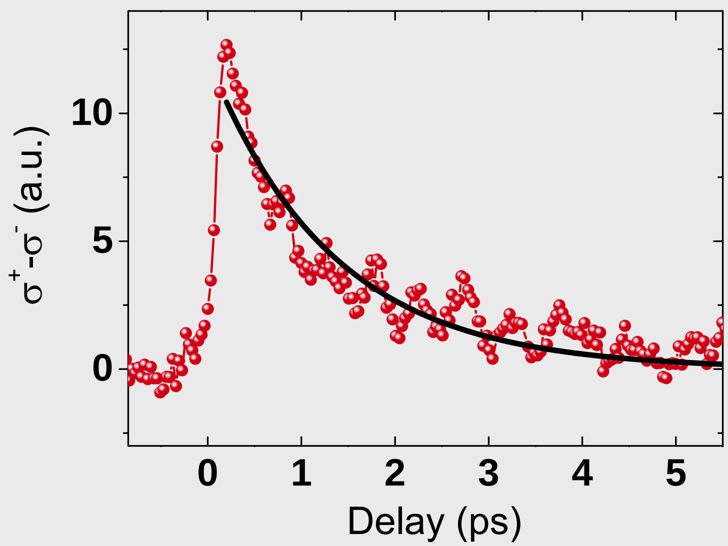

- Signal sensitive to bulk due to large penetration depth of light
- Oscillation frequency is 2.13 THz from coherent vibrations of the A_{1g} longitudinal optical phonons of Bi_2Se_3
- Exponentially decay with a characteristic time of 1.3 ps

Jean Besbas et al. (under review)

No spin momentum locking

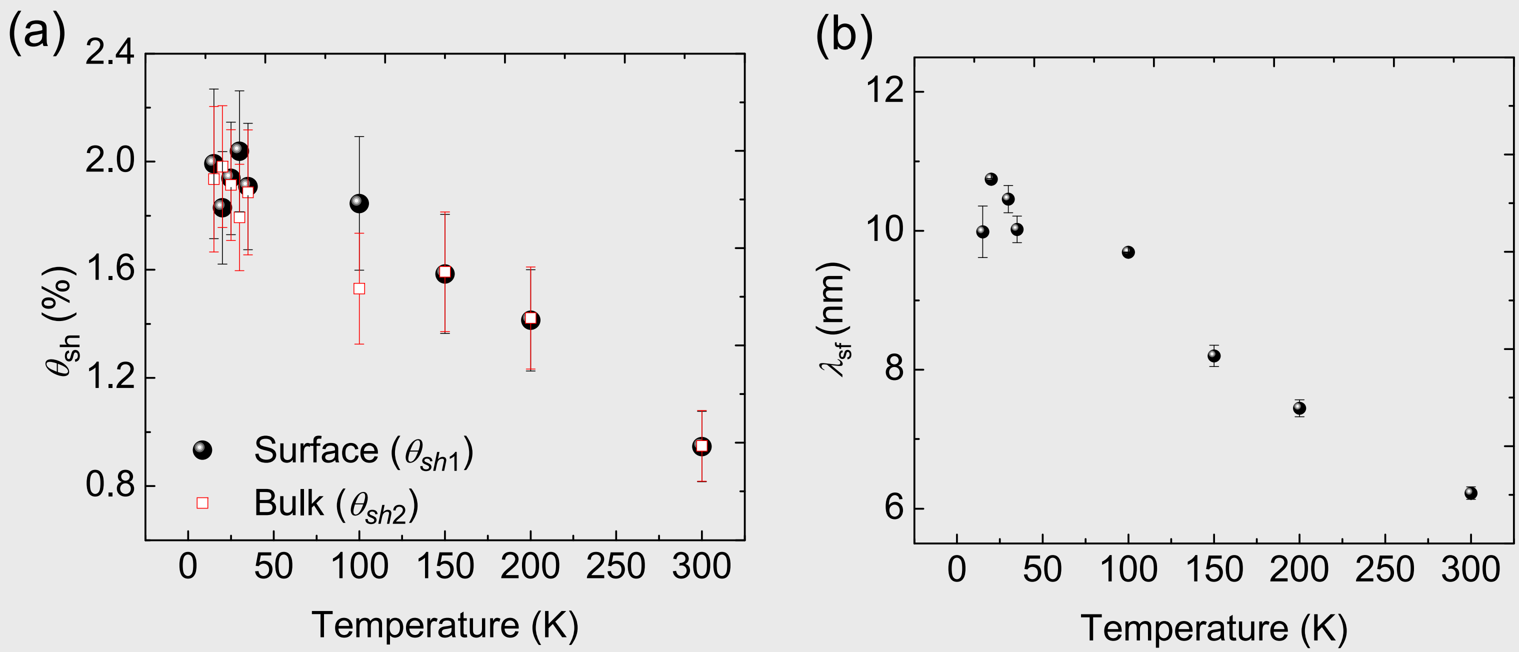

- Assumed spin Hall angle at opposite surfaces was taken to be of opposite signs.
- Spin Hall angle does not show any clear distinction between the surface and bulk value
- Momentum locking signature is not detected.

Phys. Rev. B **90**, 094403 (2014)

Comparison with other reports

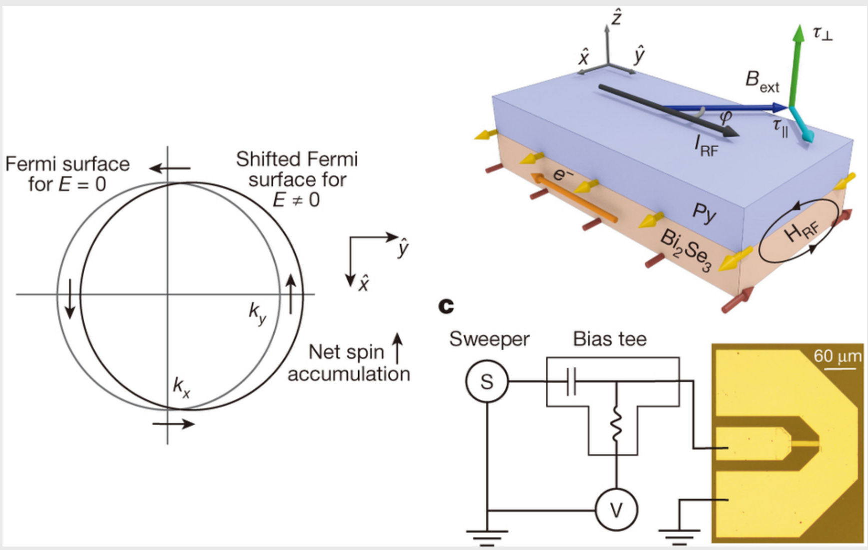

Nature **511**, 449 (2014)

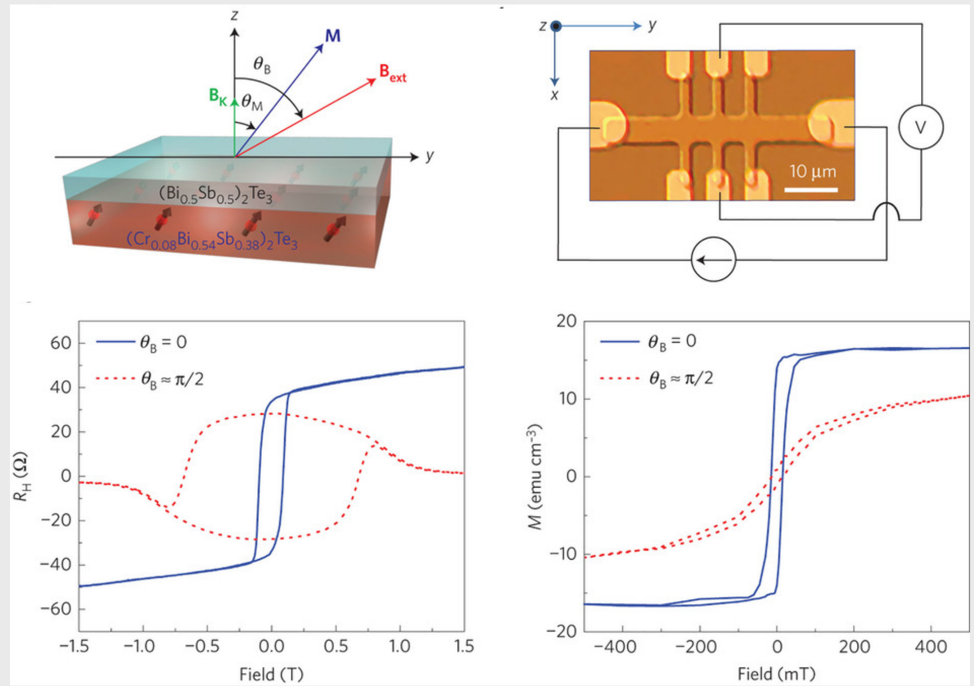

Nat. Mater. **13**, 699 (2014)

Spin torque ferromagnetic resonance measurements ➔ $\theta_{SH} = 2.0 – 3.5$

Magnetization switching by current induced spin orbit torque ➔ $\theta_{SH} = 140 – 425$

In these experiments, a charge current flows through the TI material, unlike ours.

NUS National University of Singapore

Properties of Bi_2Se_3 and $Bi_2Se_3/Co_{40}Fe_{40}B_{20}$

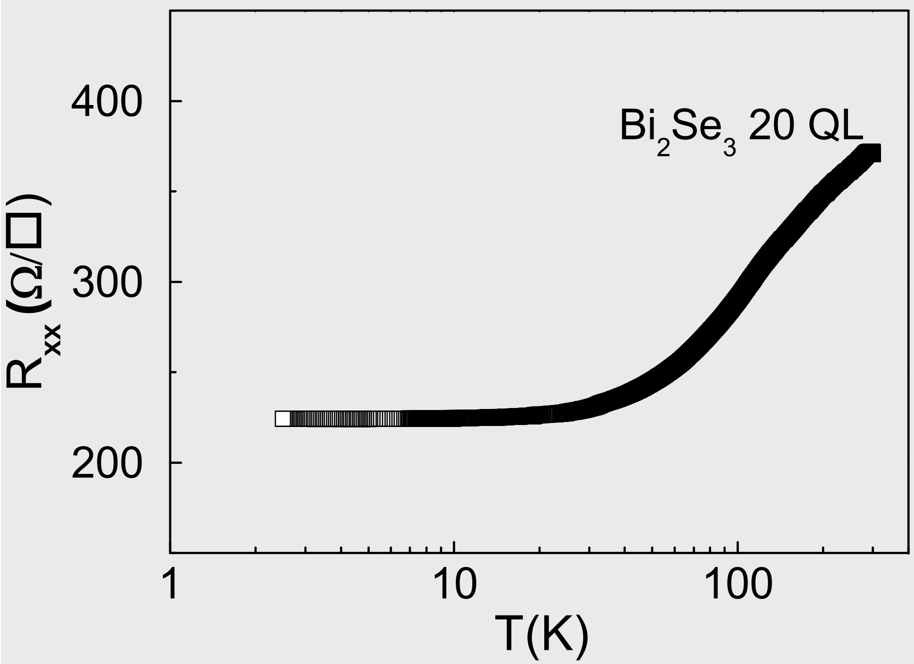

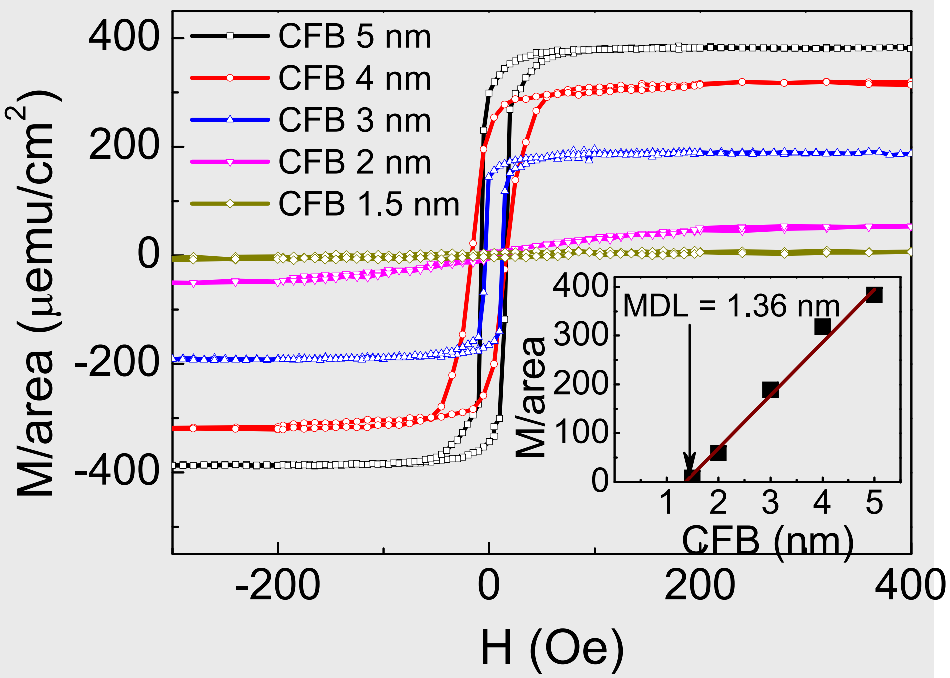

- 20 QL Bi_2Se_3 films on Al_2O_3 (0001) by MBE.
- A typical feature of resistivity saturation below 30 K for Bi_2Se_3.
- The $Co_{40}Fe_{40}B_{20}$ (CFB) dead layer ~1.36 nm.

Wang *et al.*, PRL **114**, 257202 (2015)

ST-FMR measurement of Bi_2Se_3/CoFeB

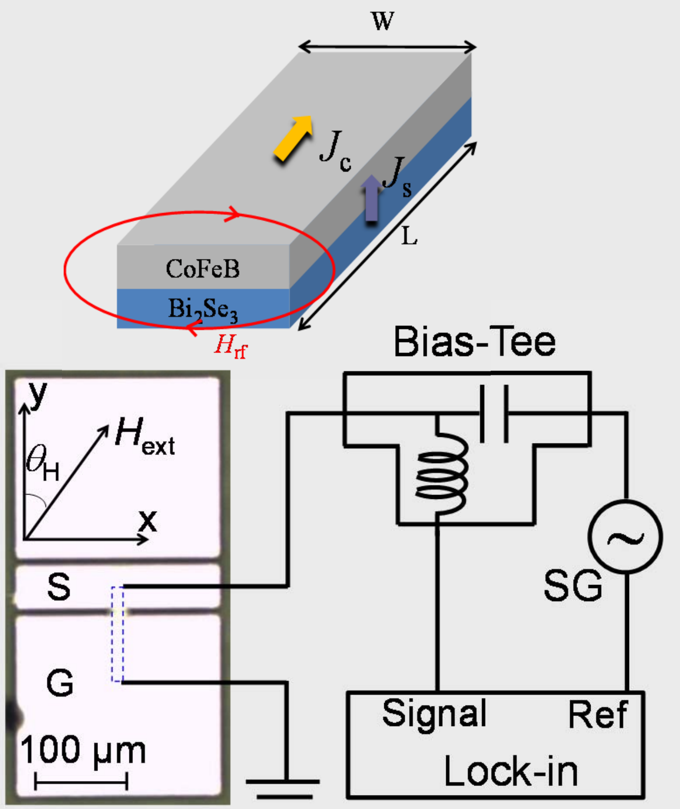

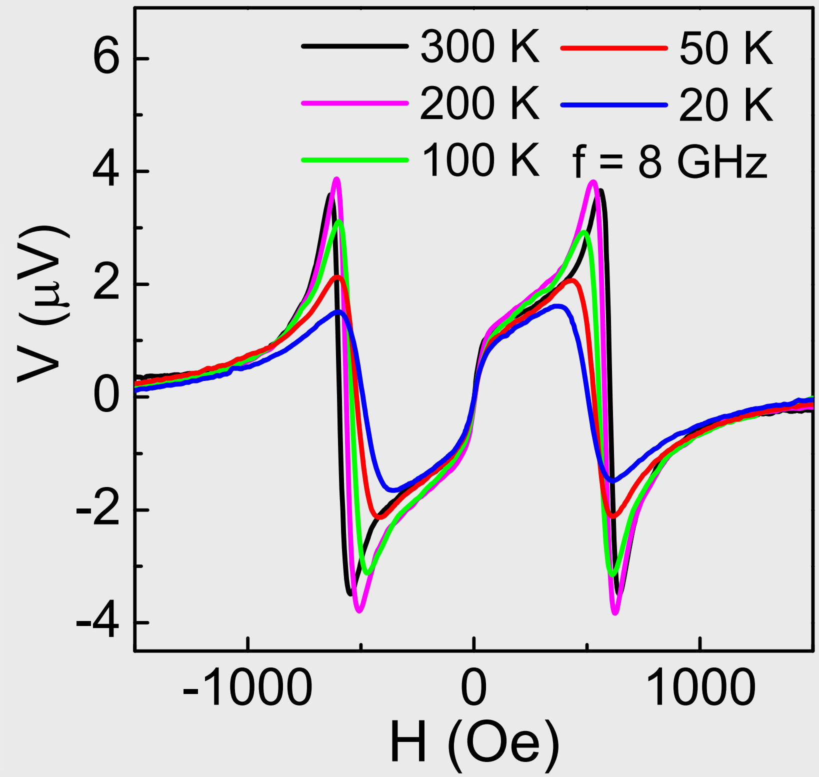

- ST-FMR measurements with a lock-in amplifier at $\theta_H = 35^\circ$.
- ST-FMR signal (V_{mix}) can be fitted by a sum of symmetric and antisymmetric Lorentzian functions:

$$V_{mix} = V_s F_{sym}(H_{ext}) + V_a F_{asym}(H_{ext})$$

V_s: in-plane torque $\tau_{||}$ on CFB
V_a: total out-of-plane torque

PRL **114**, 257202 (2015)

Two analysis methods

If only Oersted field induced out-of-plane torque (τ_{Oe}) contributes to V_a

1st method: from V_s/V_a

$$\theta_{\|} = (V_s/V_a)(e\mu_0 M_s t d/\hbar)[1+(4\pi M_{eff}/H_{ext})]^{1/2}$$

Thickness of Bi_2Se_3

2nd method: from only V_s and only V_a separately

$$V_s = -(I_{rf}\gamma \cos\theta_H/4)(dR/d\theta_H)\tau_{\|}(1/\Delta)F_{sym}(H_{ext})$$

$$\sigma_{s\|} = J_s/E = \tau_{\|} M_s t/E \qquad \theta_{\|} = \sigma_{s\|}/\sigma$$

$$V_a = -(I_{rf}\gamma \cos\theta_H/4)(dR/d\theta_H)(\Delta\tau + \tau_{Oe})\{[1+(\mu_0 M_{eff}/H_{ext})]^{1/2}/\Delta\}F_{asym}(H_{ext})$$

$$\sigma_{s\perp} = J_s/E = \Delta\tau M_s t/E \quad \theta_{\perp} = \sigma_{s\perp}/\sigma$$

Liu *et al.*,Phys. Rev. Lett. **106**, 036601 (2011)

Mellnik *et al.*, Nature **511**, 449 (2014)

Wang *et al.*, Phys. Rev. Lett. **114**, 257202 (2015)

NUS National University of Singapore

In-plane spin-orbit torque ratio in Bi_2Se_3/CoFeB

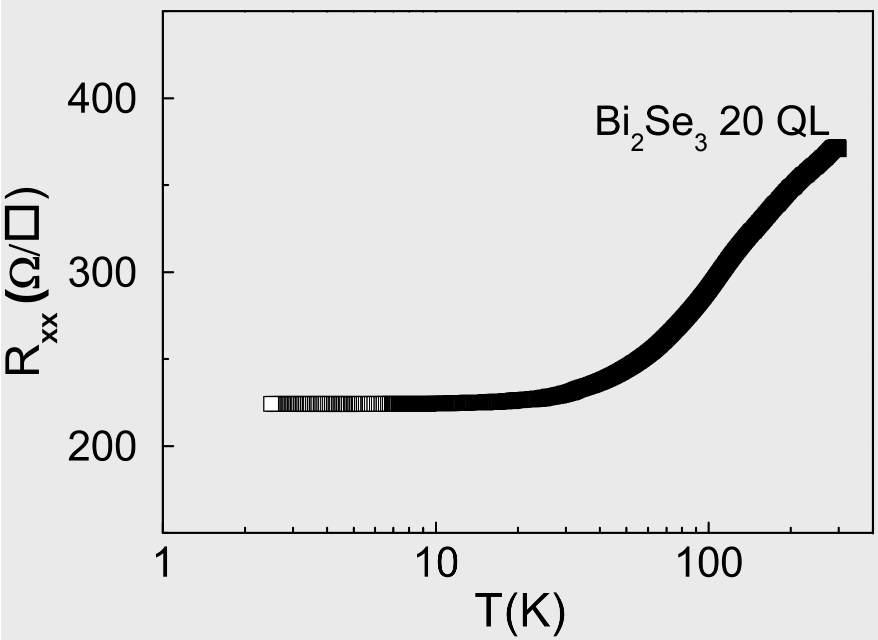

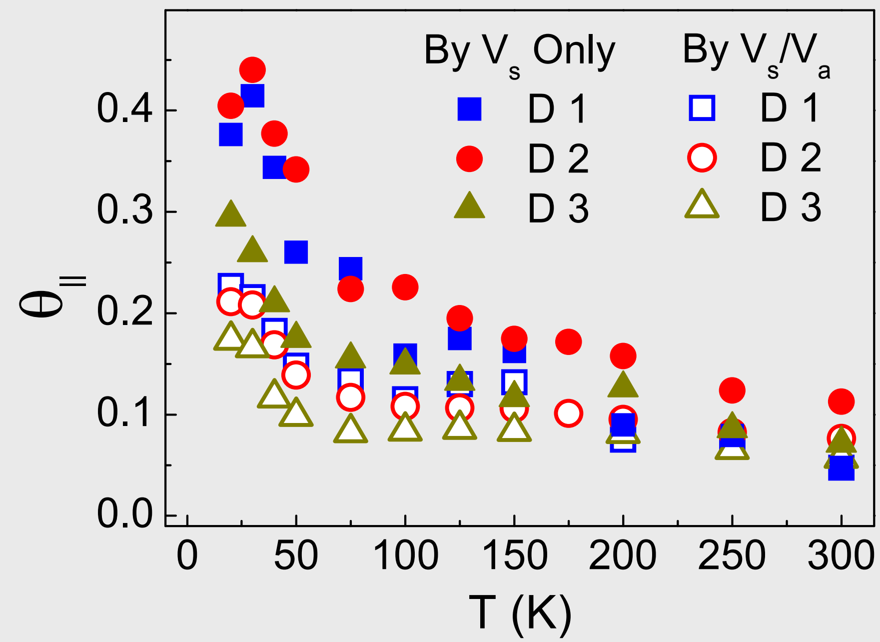

- $\tau_{||}$ ($\theta_{||}$) increases steeply and nonlinearly to **~ 0.42** at low temperature and could be almost 10 times larger than that at 300 K.
- The polarization direction of $\tau_{||}$ is consistent with spin-momentum-locked TSS.
- $\theta_{||}$ by 1^{st} and 2^{nd} methods shows a significant difference below ~ 50 K, other out-of-plane torque may contribution besides τ_{Oe}.

Wang *et al.*, PRL **114**, 257202 (2015)

In-plane spin-orbit torque (ratio) in Bi_2Se_3

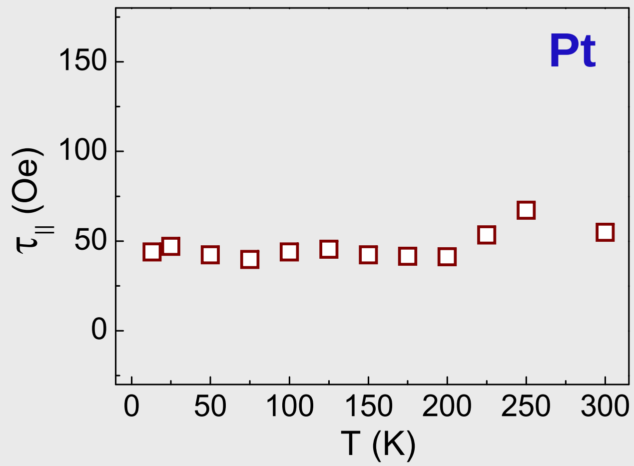

Wang *et al*., PRL **114**, 257202 (2015)

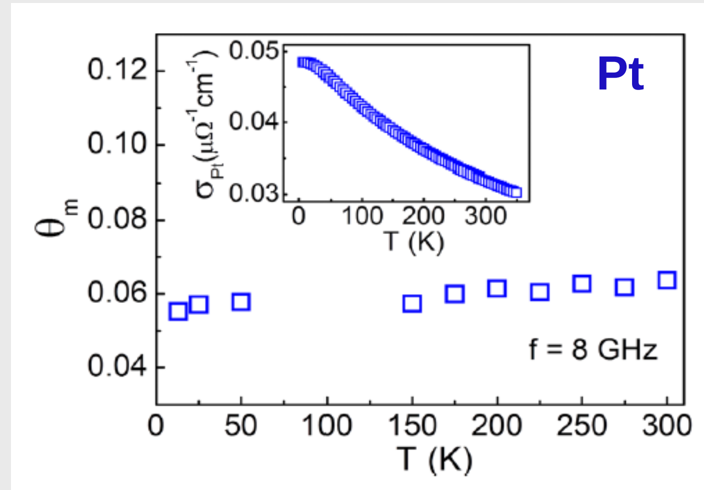

Wang *et al*., APL **105**, 152412 (2014)

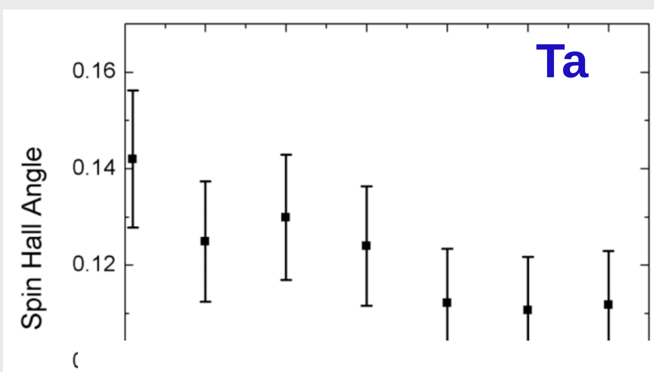

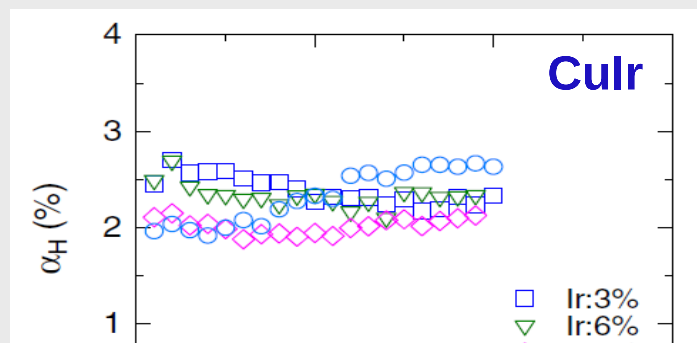

- ❑ Spin Hall mechanism from Bi_2Se_3 bulk is not the main mechanism for the nonlinear increase of $\tau_{||}$ ($\theta_{||}$) in Bi_2Se_3.
- ❑ The direction of spin polarization is consistent with TSS of TIs.

Out-of-plane spin-orbit torque ratio in Bi_2Se_3/CoFeB

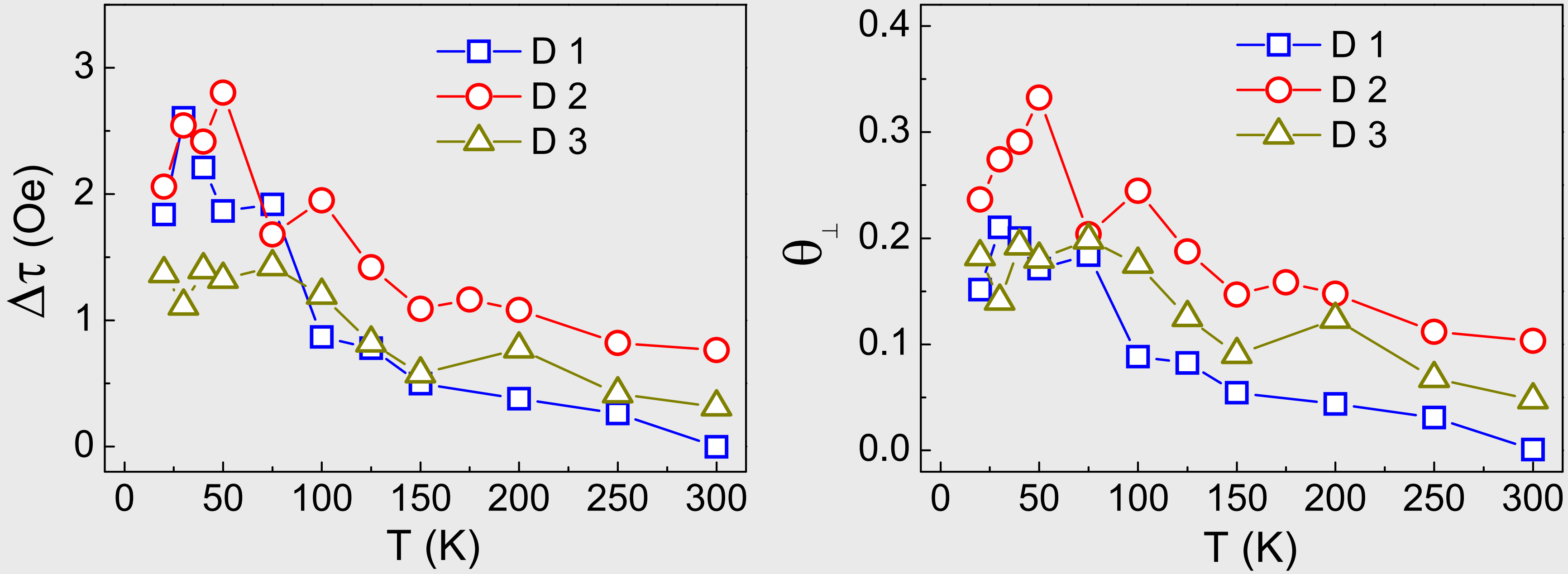

- $\Delta\tau$ ($\theta_{\perp}$) also increases at low temperature similar to $\tau_{||}$ ($\theta_{||}$).
- Rashba-split state in 2DEG of Bi_2Se_3 is not the main mechanism for $\Delta\tau$.
- Hexagonal warping in the TSS of Bi_2Se_3 can account for $\Delta\tau$ ($\theta_{\perp}$).

Wang *et al*., PRL **114**, 257202 (2015)

Is Rashba effect responsible for out-of-plane spin-orbit torque?

Metal & 2DEG in semiconductor: $H_T = \alpha_R / \hbar (\hat{z} \times k)$ Nat. Mater. **9** 230 (2010)

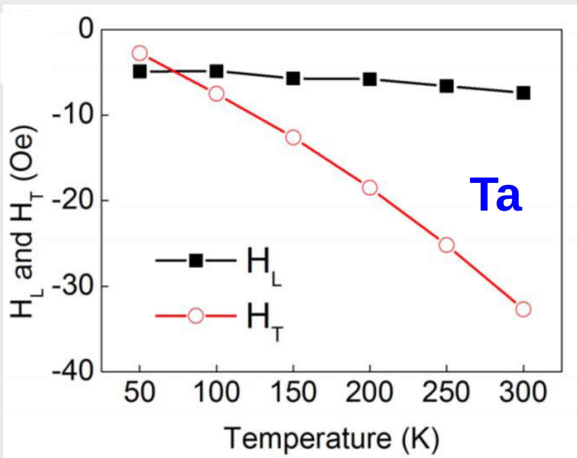

Sci. Rep. **4**, 4491 (2014)

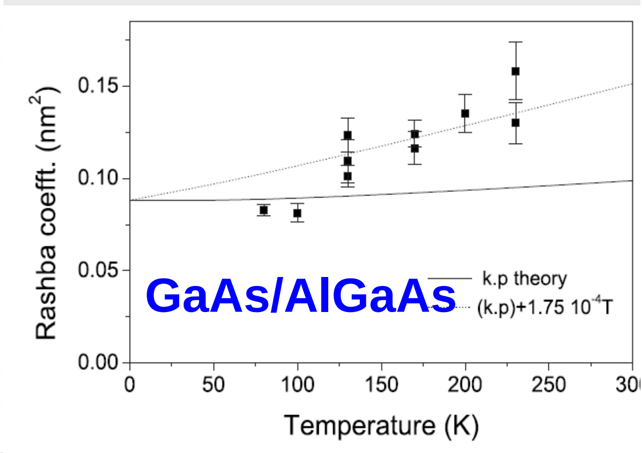

PRB **77**, 125344 (2008)

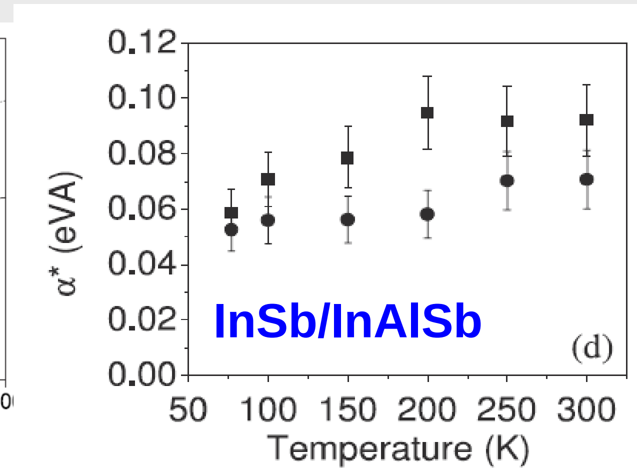

JPCM **23** 035801 (2011)

Previous Rashba reports showed a smaller effect at low temperatures.

But, we observed larger effects ($\theta_\perp$) at low temperatures.

→ Rashba effect might not be the main mechanism for $\Delta\tau$ *and* $\theta_\perp$.

NUS National University of Singapore

Out-of-plane torque in Bi_2Se_3

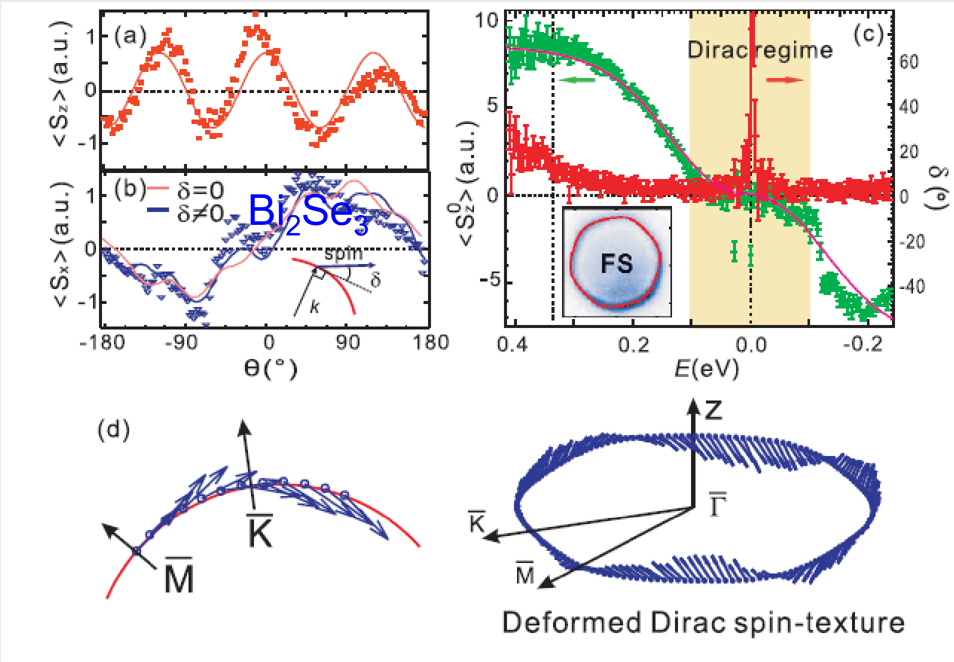

Wang *et al.*, PRL **107**, 207602 (2011)

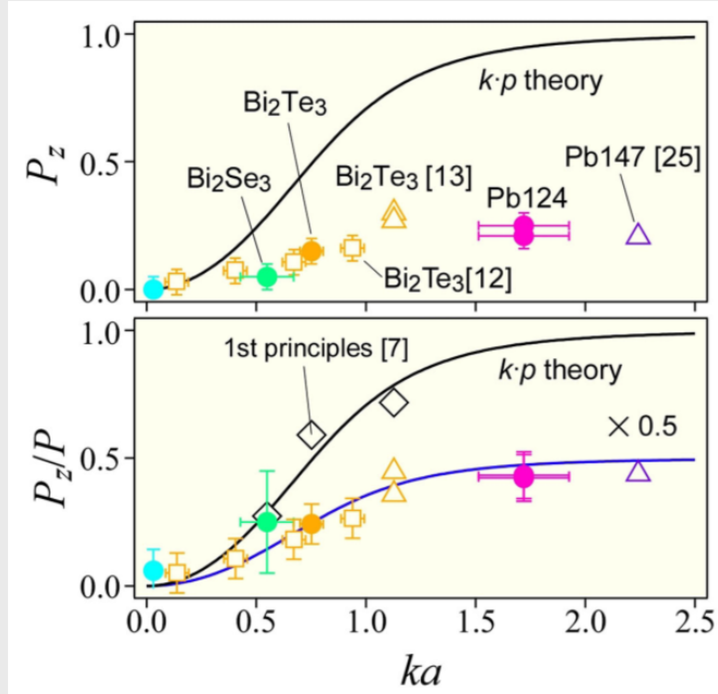

Nomura *et al.*, PRB **89**, 045134 (2014)

-Recent reports showed there is substantial out-of-plane spin polarization due to Hexagonal warping.

-**Hexagonal warping** in the TSS of Bi_2Se_3 can account for $\Delta\tau(\theta_\perp)$.

Estimation of $\theta_{||}$ from topological surface states (TSS)

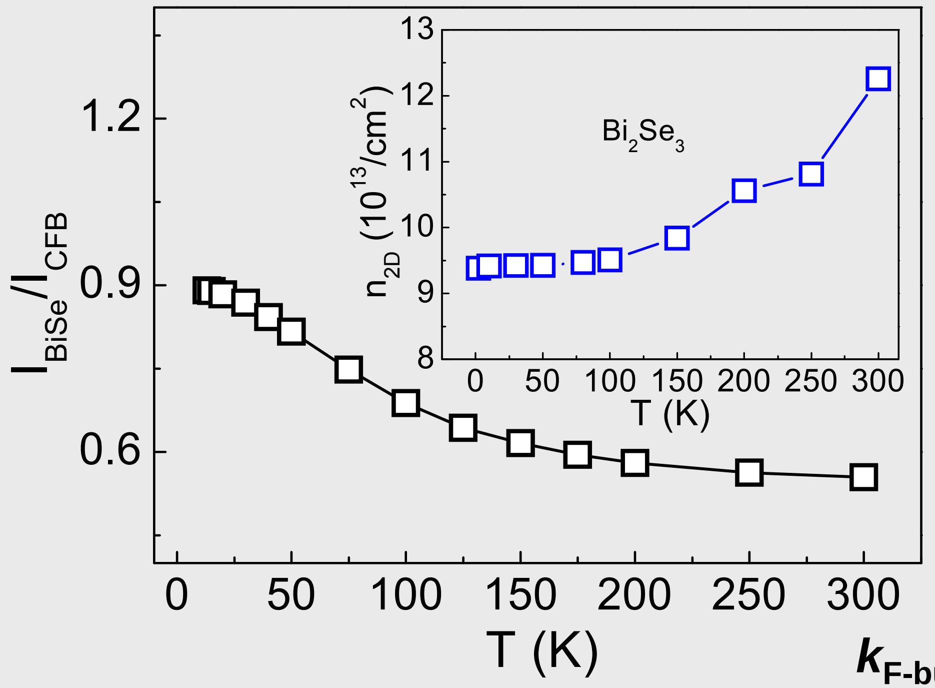

$k_{F\text{-}TSS}$ ~ 0.14 – 0.17 Å^{-1}

$k_{F\text{-}2DEG}$ ~ 0.1 – 0.12 Å^{-1}

$$n_{2D} = 2n_{TSS} + 2n_{2DEG} + n_{bulk} d$$

n_{TSS} ~ 1.56 − 2.3×10^{13} cm^{-2}

n_{2DEG} ~ 1.59 − 2.3×10^{13} cm^{-2}

n_{bulk} ~ 1 − 3.1×10^{19} cm^{-3}
(~ 1 − 3.1×10^{13} cm^{-2})

$k_{F\text{-}bulk}$ ~ 0.066 – 0.097 Å^{-1}

$k_{F\text{-}bulk} < k_{F\text{-}2DEG} < k_{F\text{-}TSS}$ and $n_{2DEG} < 2\, n_{TSS}$

By estimating $I_{TSS}:I_{2DEG}:I_{bulk}$, **$\theta_{||}$ from only TSS** at low temperature is **~ 2.1 ± 0.39** (with bulk contribution) **~ 1.62 ± 0.18** (without bulk contribution)

If we assume TSS thickness ~ 1 nm, the 2D spin orbit torque efficiency
λ_{SOT} ~ 0.8-1.05 nm.
λ_{IREE} ~ 0.2-0.33 nm in Ag/Bi interface [Nat. Commun. **4**, 2944 (2013)]

NUS National University of Singapore

Wang *et al.*, PRL **114**, 257202 (2015)

Exotic spin Hall angles from topological insulators

spin Hall angle (θ_{SH}) = 2~3.5
ST-FMR (Cornell)

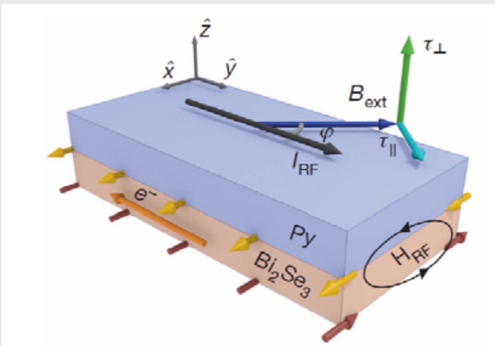

Nature **511**, 449 (2014)

θ_{SH} = 2 (low temp)
ST-FMR (NUS)

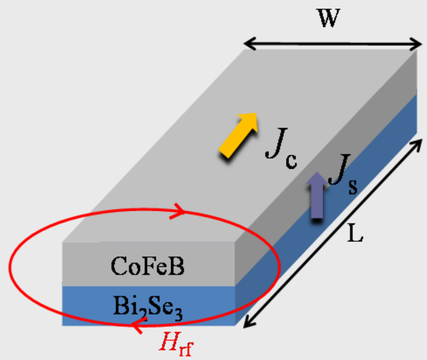

PRL **114**, 257202 (2015)

θ_{SH} = 140-425 (low temp)
spin-orbit switching (UCLA)

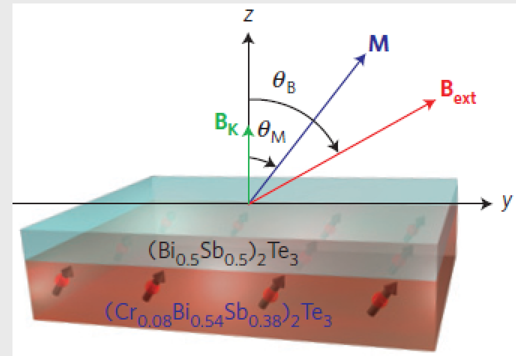

Nat. Mater. **13**, 699 (2014)

θ_{SH} = 0.01
Spin-pumping (Tohoku)

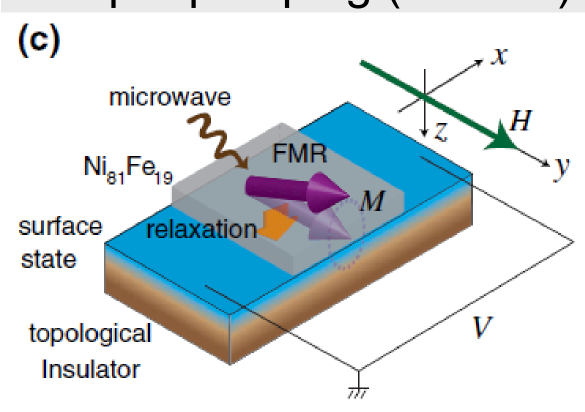

PRL **113**, 196601 (2014)

θ_{SH} = 0.01
Spin-pumping (NUS)

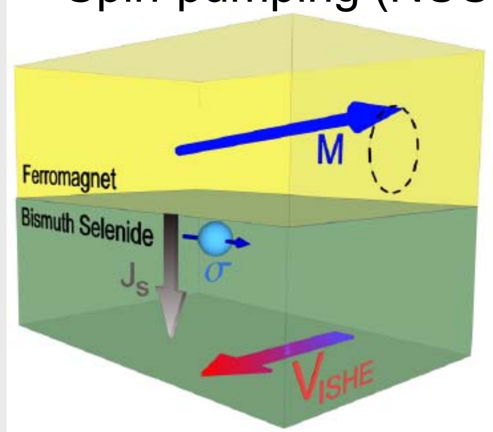

PRB **90**, 094403 (2014)

θ_{SH} = 0.01-0.4
Spin-pumping (Minnesota)

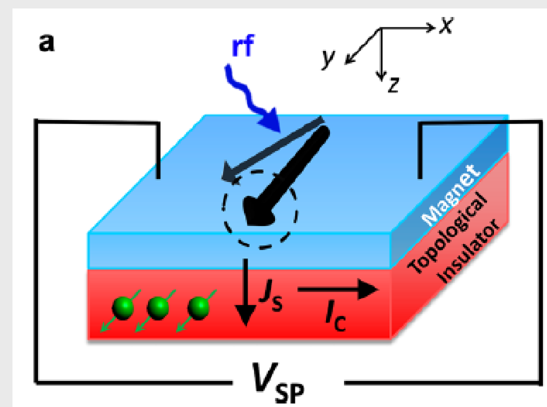

Nano Lett **15**, 7126 (2015)

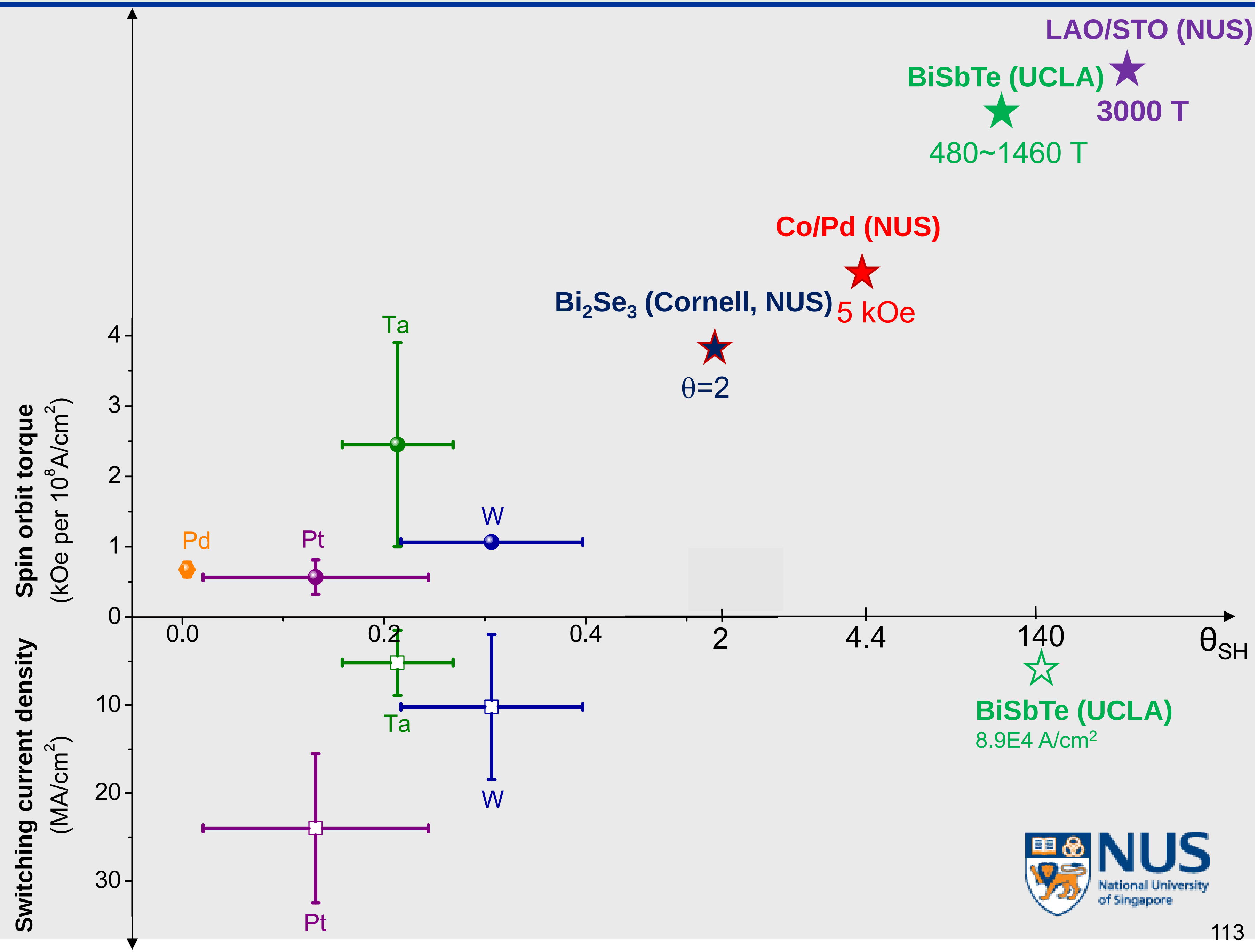
LAO/STO (NUS)
BiSbTe (UCLA)
3000 T
480~1460 T
Co/Pd (NUS)
Bi2Se3 (Cornell, NUS)
5 kOe
θ=2
Ta
W
Pd
Pt
Spin orbit torque
(kOe per 10^8 A/cm^2)
Switching current density
(MA/cm^2)
0
1
2
3
4
10
20
30
0.0
0.2
0.4
2
4.4
140
θSH
BiSbTe (UCLA)
8.9E4 A/cm2
NUS National University of Singapore

Open questions

- Why is the spin Hall angle so different from spin pumping, ST-FMR, and optical imaging measurements?
  - Spin pumping, photovoltage – bulk dominant
  - ST-FMR – surface dominant
- Are spin currents from TI big enough to switch 3d ferromagnets?
- Is there any compensation of spin orbit torques from the surface states and Rashba 2DEG?
- Can we realize a room temperature spin orbit torque TI devices?

Coexistence of surface states and Rashba bands

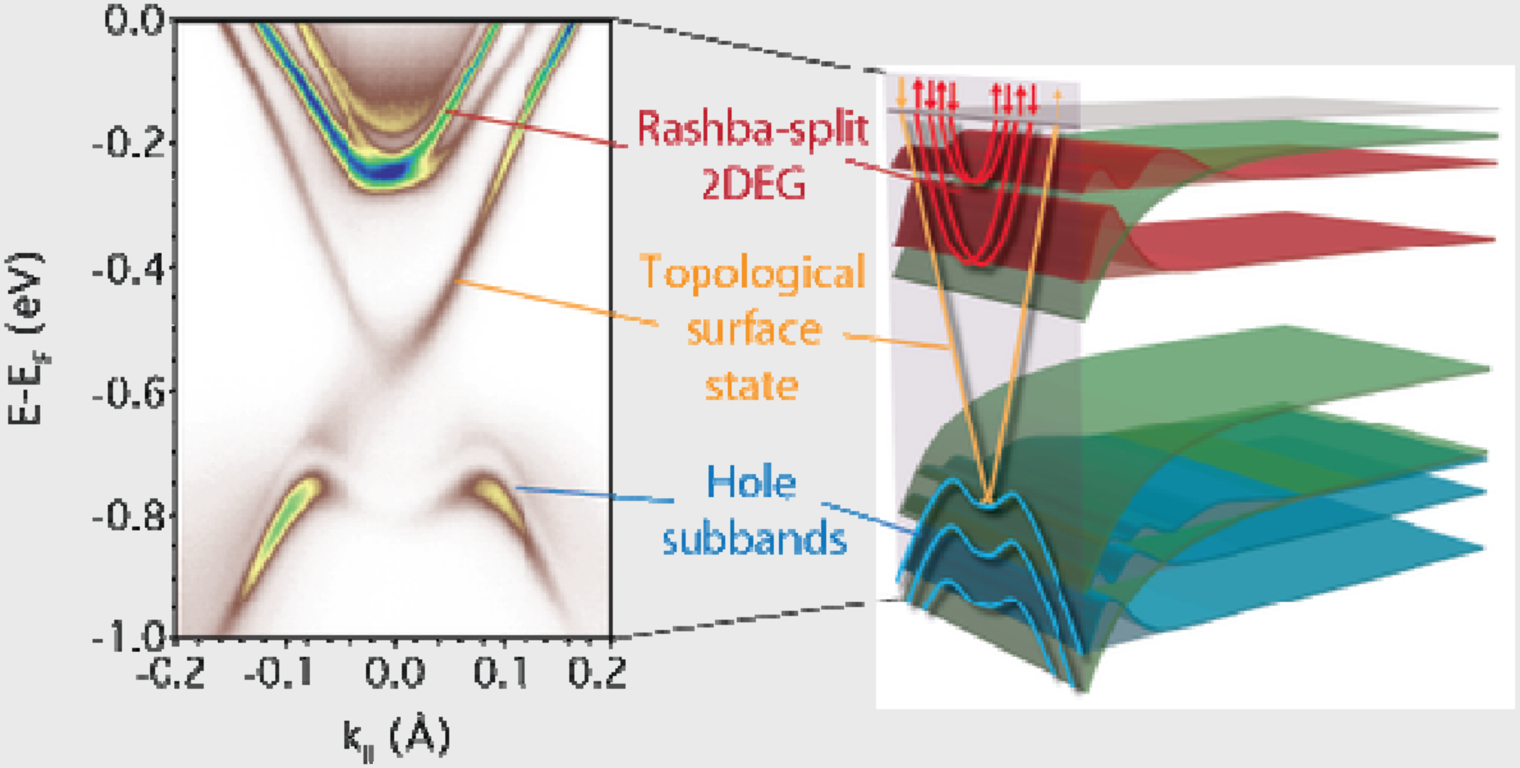

Dr. Yi Wang

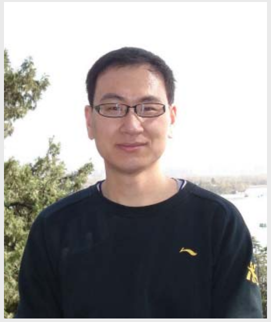

Praveen Deorani

Dr. Xuepeng Qiu

Dr. K. Narayanapillai

Li Ming Loong

Jiawei Yu

T. Venkatesan (NUS)
Seah Oh (Rutgers)
Aurelien Manchon (KAUST)
K-J. Lee (Korea Univ.)